CHALMERS
UNIVERSITY OF TECHNOLOGY

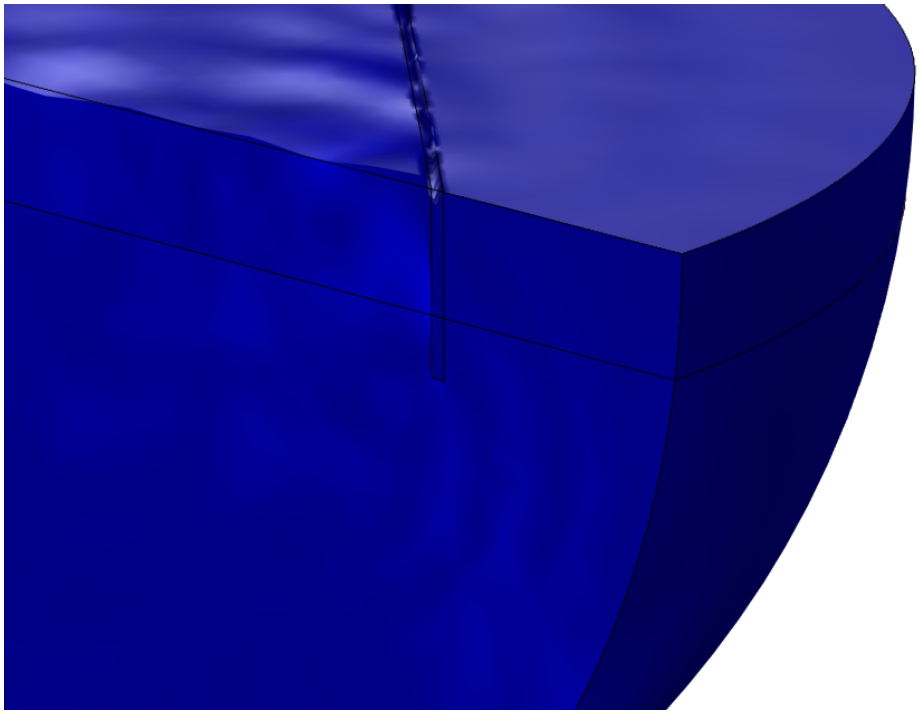

Reflection, absorption and filtering of ground vibrations

A study in the use of different arrays of cylinders
to attenuate and filter ground vibrations

Master's thesis in Master Programme Sound and Vibration

ALEXANDER SANDERCOCK

Department of Civil and Environmental Engineering
Chalmers University of Technology
Gothenburg, Sweden 2017

Master's thesis BOMX02-16-161

Reflection, absorption and filtering of ground vibrations

A study in the use of different arrays of cylinders
to attenuate and filter ground vibrations

ALEXANDER SANDERCOCK

CHALMERS
UNIVERSITY OF TECHNOLOGY

Department of Civil and Environmental Engineering
Division of Applied Acoustics
Chalmers University of Technology
Gothenburg, Sweden 2017

Reflection, absorption and filtering of ground vibrations
A study in the use of different arrays of cylinders to attenuate and filter ground vibrations
ALEXANDER SANDERCOCK

Supervisor: Patrik Höstmad, Division of Applied Acoustics
Examiner: Patrik Höstmad, Division of Applied Acoustics

Master's thesis BOMX02-16-161
Department of Civil and Environmental Engineering
Division of Applied Acoustics
Chalmers University of Technology
SE-412 96 Gothenburg
Telephone +46 31 772 1000

Cover: The refraction and reflection of incoming ground vibrations at the interface of a trench, constructed in COMSOL.

Typeset in LaTeX
Printed by Chalmers University of Technology
Gothenburg, Sweden 2017

Reflection, absorption and filtering of ground vibrations
A study in the use of different arrays of cylinders to attenuate and filter ground vibrations
Alexander Sandercock
Department of Civil and Environmental Engineering
Chalmers University of Technology

Abstract

With the increased rate of urbanization comes an increase in disturbing ground vibrations. These can be produced by building operations, different kinds of traffic and in some cases mining and military operations. It is therefore necessary to try and reduce the amplitude of these disturbing, and in extreme cases damaging vibrations.
This thesis investigates different wave barrier types in different ground types, with the aim being to find the optimal filter for frequencies below 20 Hz. There are established methods which can reduce the velocity of surface ground vibrations, which include underground walls, trenches and treatment of the ground. These methods, however, can be expensive to implement as they all require extensive groundwork operations which are both disturbing to the surrounding populace and costly. Different arrays of hollow cylinders acting as a barrier in the wavefronts path were therefore studied. This was performed by simulating these barriers in a 3D halfspace in an FEM model to see if any reduction of the velocity level at the surface could be measured below 20 Hz. The model was entirely homogeneous and no attempt was made at changing different ground parameters such as porosity or moisture content. Despite investigating 7 different array types in 3 ground types there was no broadband reduction below 20 Hz, only narrowband reduction at individual frequencies, often above 20 Hz. After these initial investigations the effect of these cylinders was briefly studied for the effect on underground vibrations, where more promising results were achieved. This suggests that in areas where the ground is soft and the surrounding structures require deep foundations, arrays of cylinders could be useful for reducing the amplitude of incoming body waves which would otherwise interact with deep foundations and cause disturbing vibrations in the building.

Keywords: Vibrations, reflection, absorption, ground, acoustics, dynamics, rayleigh, waves.

Reflektion, absorption och filtrering av markvibrationer
En studie i användningen av olika uppsättningar av cylindrar för att dämpa och filtrera markvibrationer.
Alexander Sandercock
Institution för Arkitektur och Samhällsbyggnadsteknik
Chalmers Tekniska Högskola

Sammanfattning

Men en ökning av urbanisering tillkommer en ökning av störande markvibrationer. Dessa produceras av bygg, trafik och i vissa fall gruv- och militär operationer. Det är viktigt att försöka minska amplituden av dessa störande och i vissa fall farliga markvibrationer.
Detta projekt gick ut på att undersöka olika vågbarriärer i olika marktyper, med syftet att hitta den optimala filter för alla frekvenser under 20Hz. Det finns beprövade metoder som kan minska hastighetsnivåerna av yt-vågor. Detta kan vara väggar under jordytan, diken och förstyvning av marken. Dock så är dessa metoder dyra och störande när de skall genomföras eftersom omfattande markarbete krävs. Flera olika uppställningar av tomma cylindrar i vågfrontens väg simulerades med Finit Element Metoden i COMSOL för att undersöka om dessa barriärer ger upphov till en amplitudminskning under 20Hz.
Modellen var homogent och inga försök gjordes för att undersöka om olika parametrar i marken, såsom porositeten eller vätskehalten ändrade propageringssättet. Trots att 7 olika barriärer studerades i 3 olika marktyper observerades ingen bredbandig minskning av amplituden av ytvågorna under 20Hz, utan bara smalbandig minskning för vissa frekvenser. Effekten av en uppsättning av tomma cylindrar på volymvågorna (vågorna under ytan) studerades med bättre resultat. Detta kan innebär att i områden där marken är av en mjukare typ och omkringliggande byggnader behöver djupa fundament, kan en uppsättning av tomma cylindrar användas för att minska amplituden av vågor som skulle annars skakar de djupa fundament.

Nyckelord: Vibrationer, reflektion, absorption, mark, akustik, dynamik, rayleigh, vågor.

Acknowledgements

I would like to thank the Division of Applied Acoustics at Chalmers University of Technology for their support throughout this project, as well as the superb education provided throughout the Master Programme Sound and Vibration. The knowledge and advice given by my supervisor, Patrik Höstmad, has been instrumental in the completion of this thesis. Chalmers has also provided me with an inspiring environment, numerous resources and great facilities in which to develop myself and to study. I have nothing but praise for this great learning institution.

My family, in particular my parents and my grandmother, have also been supportive throughout my entire education, and have always helped me set my goals high. Without their encouragement throughout my five years of University, it would have been a much more difficult journey.

My closest friends; Victor Neugebauer and Benjamin Oakes, both fellow engineers, have also inspired me to improve my intellect throughout the years I have known them, while having fun along the way.

I would also like to thank my girlfriend, Xenia Sokolova, who has been there for me and helped me handle difficult periods throughout my studies, for which I am very grateful.

List of Figures

List of Tables

Contents

1 Introduction

The geodynamic effects caused by non-siesmic phenomena, such as construction, mining, logistics and to a lesser extent military operations and exercises, have become an increasingly important issue with the expansion of society.
The increased urbanization and expansion of cities has led to the construction of large infrastructure and housing projects in close proximity to heavily populated areas. The foundation work for these projects can involve blasting and piling, causing ground vibrations which can be disturbing to the local populace. In some cases these disturbing vibrations can lead to law suits.
Another effect of increasing urbanization is an increase of traffic, both on roads and railways, along with the allowance of heavier loads and higher speeds. This increases the risk of disturbing vibrations to areas around critical logistical infrastructure.
Mining operations use explosives to expand existing mines in order to extract more ore. Mines are normally located further away from densely populated areas, but the size of the blasts (often involving many tons of explosives) can mean that population centers which are relatively far away from these operations can still be disturbed by the generated ground vibrations.
Military operations and weapons testing, while involving smaller explosions than mining operations, can also cause significant disturbance to the surrounding area.

1.1 Purpose

The purpose of this thesis is to determine if it is possible to filter ground vibrations using an array of cylinders in the wave fronts path. This will be determined through simulations using Finite Element Method (FEM) and through measurements.

1.2 Aims and questions

The aims of this thesis are as follows:

- To produce a theoretical and mathematical framework to test if the theory works. This can be through analytical calculations or numerical simulations.
- To test the theory in real world conditions and compare the measured results to the theoretical and mathematical framework.
- To optimize any solution to maximize the cost to benefit ratio.
- Analyse any potential use for the method in question.

1.3 Limitations of the study

Large bodies of ground are usually very an-isotropic and in-homogeneous by nature. As it is strictly the propagation and attenuation of different wave types around different wave barriers that is being studied the elastic half space was assumed to be homogenous and isotropic. There are a number of other variables that effect the ground in real world conditions which were not considered[1]:

- Moisture content.
- Porosity.

- Average particle size.
- Wet and dry density.
- Packing grade.
- Particle size distribution

These variables can affect the wave propagation through the ground, mainly through changing the material properties which change the propagation velocity and material damping.

1.4 This reports disposition

In order to give the reader a clear understanding of the topic, a large part of this report is dedicated to the theory of ground vibrations. Wave propagation through an infinite elastic medium and an elastic half space is therefore covered in detail before moving on to wave propagation in layered systems. Lastly wave attenuation in the ground is discussed, both the theory and the established methods of dealing with ground vibrations.
The set up of the Finite Element Model is then discussed to give the reader a good understanding of why and how the model was made, as well as discussing the different ground and barrier types that will be simulated.
The results of the simulations are then presented, first for each individual barrier type, and then compiled into one table to allow the reader to compare all of the barrier types. A small subsection finished off this section by looking at the effects of these barrier types on underground waves.
The project and its results are then discussed. In this section different ideas as to why the results were not as expected were discussed as well as ideas for future research and a new hypothesis as to what could produce better results. Improvements to the methodolgy of this project has also been discussed.
The final section is the conclusion, where the results are compared to the aims of this project, and more future research is discussed.
At the end of this report the reader will find the bibliography and the appendix with the Matlab code.

2 Theory

2.1 Wave propagation in an infinite, elastic, homogenous, isotropic medium

In order to describe the motion of waves in an infinite, elastic, homogenous, isotropic medium, the solutions to the equation of motion in three dimensions must be found.
To begin with, the equilibrium of an infinitely small element, such as in figure 1 must be studied. The stresses on each face are represented by sets of orthogonal vectors. [2]

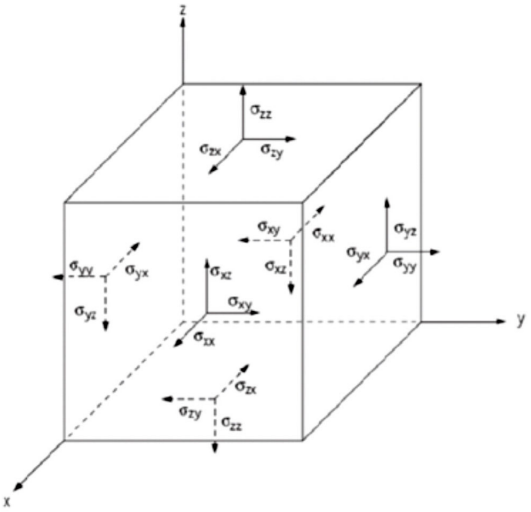

Figure 1: Figure showing 3-dimensional stress state on a small element, with normal and shear stress components in tensor notation. Stress is a second order tensor. [3]

This shows three normal stresses σ_{xx}, σ_{yy} and σ_{zz}, and six shear stresses σ_{xy}, σ_{yx}, σ_{xz}, σ_{zx}, σ_{yz} and σ_{zy}. The equilibrium equations in every dimension can then be assembled of the appropriate vectors from 1. In the x-direction the vectors have the following stress values:

$$\sigma_{xx} = (\sigma_x + \frac{\partial \sigma_x}{\partial x}\Delta x)\Delta y \Delta z \tag{1a}$$

$$\sigma_{xy} = (\tau_{xy} + \frac{\partial \tau_{xy}}{\partial y}\Delta y)\Delta x \Delta z \tag{1b}$$

$$\sigma_{xz} = (\tau_{xz} + \frac{\partial \tau_{xz}}{\partial z}\Delta z)\Delta x \Delta y \tag{1c}$$

The equilibrium equation for the x-direction can then be assembled using equations 1a,1b,1c and their reciprocals to form equation 2.

$$(\sigma_x + \frac{\partial \sigma_x}{\partial x}\Delta x)\Delta y\Delta z - \sigma_{xx}\Delta y\Delta z + (\tau_{xy} + \frac{\partial \tau_{xy}}{\partial y}\Delta y)\Delta x\Delta z$$
$$- \tau_{xy}\Delta x\Delta z + (\tau_{xz} + \frac{\partial \tau_{xz}}{\partial z}\Delta z)\Delta x\Delta y - \tau_{xz}\Delta x\Delta y = 0 \quad (2)$$

The equilibrium equations can then be written for the y and z directions in the same manner. Applying Newtons second law and neglecting the body forces in the x-direction gives the equation of motion in terms of stresses as:

$$\left(\frac{\partial \sigma_{xx}}{\partial x} + \frac{\partial \tau_{xy}}{\partial y} + \frac{\partial \tau_{xz}}{\partial z}\right)\Delta x\Delta y\Delta z = \rho(\Delta x\Delta y\Delta z)\frac{\partial^2 u}{\partial t^2} \quad (3)$$

Equation 3 can also be written for the y- and z-directions. The equations of motions in all three directions can then be written as:

$$\rho\frac{\partial^2 u}{\partial t^2} = \frac{\partial \sigma_{xx}}{\partial x} + \frac{\partial \tau_{xy}}{\partial y} + \frac{\partial \tau_{xz}}{\partial z} \quad (4a)$$
$$\rho\frac{\partial^2 v}{\partial t^2} = \frac{\partial \tau_{yx}}{\partial x} + \frac{\partial \sigma_{yy}}{\partial y} + \frac{\partial \tau_{yz}}{\partial z} \quad (4b)$$
$$\rho\frac{\partial^2 w}{\partial t^2} = \frac{\partial \tau_{zx}}{\partial x} + \frac{\partial \tau_{zy}}{\partial y} + \frac{\partial \sigma_{zz}}{\partial z} \quad (4c)$$

Where the notations u, v and w denote the displacements in the x, y and z directions respectively. The following relations for an elastic medium can then be inserted into equations 4 in order to express the right hand sides in terms of displacements:

$$\sigma_{xx} = \lambda\overline{\epsilon} + 2G\epsilon_x \qquad \tau_{xy} = \tau_{yx} = G\gamma_{xy} \quad (5a)$$
$$\sigma_{yy} = \lambda\overline{\epsilon} + 2G\epsilon_y \qquad \tau_{yz} = \tau_{zy} = G\gamma_{yz} \quad (5b)$$
$$\sigma_{zz} = \lambda\overline{\epsilon} + 2G\epsilon_z \qquad \tau_{zx} = \tau_{xz} = G\gamma_{zx} \quad (5c)$$

where;

$$G = \frac{E}{2(1+\nu)} \qquad \lambda = \frac{\nu E}{(1+\nu)(1-2\nu)} \quad (6)$$

Where ν is Poissons ratio, λ is the Young's modulus for stress and G is the shear modulus. $\overline{\epsilon}$ is the dilation, or volume expansion, and is defined as:

$$\overline{\epsilon} = \epsilon_x + \epsilon_y + \epsilon_z \quad (7)$$

The relationships for strain and rotation is terms for displacement for each dimension then

become:

$$\epsilon_x = \frac{\partial u}{\partial x} \qquad \gamma_{xy} = \frac{\partial v}{\partial x} + \frac{\partial u}{\partial y} \qquad 2\overline{\omega_x} = \frac{\partial w}{\partial y} - \frac{\partial v}{\partial z} \tag{8a}$$

$$\epsilon_y = \frac{\partial v}{\partial y} \qquad \gamma_{yz} = \frac{\partial w}{\partial y} + \frac{\partial v}{\partial z} \qquad 2\overline{\omega_y} = \frac{\partial u}{\partial z} - \frac{\partial w}{\partial x} \tag{8b}$$

$$\epsilon_z = \frac{\partial w}{\partial z} \qquad \gamma_{zx} = \frac{\partial u}{\partial z} + \frac{\partial w}{\partial x} \qquad 2\overline{\omega_z} = \frac{\partial v}{\partial x} - \frac{\partial u}{\partial y} \tag{8c}$$

Where ϵ_x, ϵ_y and ϵ_z are the linear expansion variables, γ_{xy}, γ_{yz} and γ_{zx} are the shear strain variables and ω_x, ω_y and ω_z are the rotational variables in each axis.
The equations of motion for an infinite homogeneous, isotropic, elastic medium can be formed by combining the expressions from equations 5c, 6 and 8c into equation 4. This gives the following expressions:

$$\rho\frac{\partial^2 u}{\partial t^2} = (\lambda + G)\frac{\partial \overline{\epsilon}}{\partial x} + G\nabla^2 u \tag{9a}$$

$$\rho\frac{\partial^2 v}{\partial t^2} = (\lambda + G)\frac{\partial \overline{\epsilon}}{\partial y} + G\nabla^2 v \tag{9b}$$

$$\rho\frac{\partial^2 w}{\partial t^2} = (\lambda + G)\frac{\partial \overline{\epsilon}}{\partial z} + G\nabla^2 w \tag{9c}$$

Where ∇^2 is the laplacian operator in cartesian coordinates.

$$\nabla^2 = \frac{\partial^2}{\partial x^2} + \frac{\partial^2}{\partial y^2} + \frac{\partial^2}{\partial z^2} \tag{10}$$

Equations 9 can be differentiated with respect to x, y and z respectively, before being added together to form:

$$\rho\frac{\partial^2 \overline{\epsilon}}{\partial t^2} = (\lambda + 2G)\nabla^2 \overline{\epsilon} \tag{11}$$

Which, after moving the ρ term to the right side becomes the exact form of the wave equation:

$$\frac{\partial^2 \overline{\epsilon}}{\partial t^2} = \nu_P^2 \nabla^2 \overline{\epsilon} \tag{12}$$

This is the first solution to the equations of motion, which represents the **compression wave**, otherwise known as the P-wave. The propagation velocity of the compression wave is ν_P^2:

$$\nu_P = \sqrt{\frac{\lambda + 2G}{\rho}} \tag{13}$$

If one differentiates the equation of motion in the y-direction, equation 9b, with respect to z, and the equation of motion in the z-direction, equation 9c, with respect to y (therefore expressing

a rotation), and cancel the dilation term, $\bar{\epsilon}$, by subtracting these two equations, gives the following term:

$$\rho\frac{\partial^2}{\partial t^2}\left(\frac{\partial w}{\partial y}-\frac{\partial v}{\partial z}\right)=G\nabla^2\left(\frac{\partial w}{\partial y}-\frac{\partial v}{\partial z}\right) \tag{14}$$

Where the term in parenthesis is equivalent to the expression for rotation in equation 8c, $\overline{\omega}$. This term can then be replaced in equation 14 to give:

$$\rho\frac{\partial^2\overline{\omega_x}}{\partial t^2}=G\nabla^2\overline{\omega_x} \tag{15}$$

$$\Rightarrow \frac{\partial^2\overline{\omega_x}}{\partial^2}=\nu_s^2\nabla^2\overline{\omega_x} \tag{16}$$

The same expressions can be obtained for $\overline{\omega_y}$ and $\overline{\omega_z}$. This rotational motion is therefore propagated with velocity:

$$\nu_s=\sqrt{\frac{G}{\rho}} \tag{17}$$

This wave type is known as a **shear wave**, or S-wave, and is the second solution to the equation of motion in an infinite elastic medium.
This shows that two wave types can be sustained in an infinite elastic medium:

- A dilational wave, or P-wave, with a push-pull partical motion parallel to the wave front.
- A distortional wave, or S-wave, with a transverse partical motion normal to the wave front.

These motions can be seen in figure 2. These wave types also have different propagation velocities; ν_p and ν_s. Meaning that they will arrive at different times to a point at a fixed distance from the point of origin.

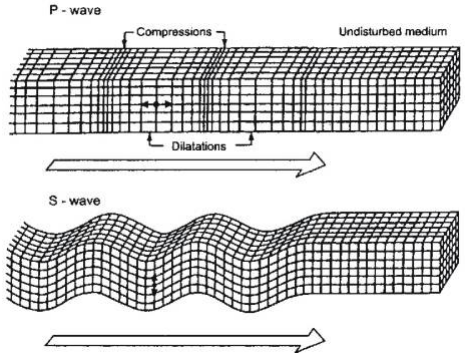

Figure 2: The motion of P- and S-waves in an infinite elastic medium. [4]

2.1.1 Surface waves in an elastic half space

In an infinite elastic medium, the solutions to the equation of motion yield two solutions; P- and S-waves. If the infinite elastic medium is given a surface, it is then known as an elastic half space. By introducing a surface, and therefore new boundary conditions for that plane, the equations of motion change; yielding a third solution. This third solution corresponds to a wave which is confined to the surface of the elastic half space. This surface wave is known as the **Rayleigh wave** (R-wave). The influence of this wave decreases rapidly with depth and frequency [5].

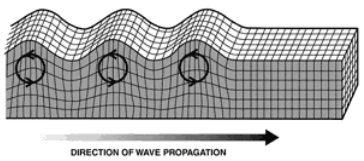

Figure 3: The motion of Rayleigh waves in an elastic half space. [6]

2.1.2 Rayleigh waves

Equations 9a, 9b and 9c can be solved for a half space by imposing the relevant boundary conditions for the free surface. The free surface is the $x-y$ plane, and z is the depth of the half space. Particle displacements of a plane wave travelling in the x-direction will be independent of the y-direction. Displacements in the x and z directions, or u and w respectively, can be written in terms of two potential functions Φ and Ψ:

$$u = \frac{\partial \Phi}{\partial x} + \frac{\partial \Psi}{\partial z} \qquad\qquad w = \frac{\partial \Phi}{\partial z} - \frac{\partial \Psi}{\partial x} \tag{18}$$

The dilation of the wave, $\overline{\epsilon}$, in respect to u and w is then:

$$\overline{\epsilon} = \frac{\partial u}{\partial x} + \frac{\partial w}{\partial z} = \frac{\partial}{\partial x}\left(\frac{\partial \Phi}{\partial x} + \frac{\partial \Psi}{\partial z}\right) + \frac{\partial}{\partial z}\left(\frac{\partial \Phi}{\partial z} - \frac{\partial \Psi}{\partial x}\right) = \nabla^2 \Phi \tag{19}$$

The rotation in the $x-z$ plane can then be represented with:

$$2\overline{\omega}_y = \frac{\partial u}{\partial z} + \frac{\partial w}{\partial x} = \frac{\partial}{\partial z}\left(\frac{\partial \Phi}{\partial x} + \frac{\partial \Psi}{\partial z}\right) - \frac{\partial}{\partial x}\left(\frac{\partial \Phi}{\partial z} - \frac{\partial \Psi}{\partial x}\right) = \nabla^2 \Psi \tag{20}$$

The potential functions, Φ and Ψ have therefore been shown to represent the dilation and rotation of the medium, respectively.
The displacements, u and w can be substituted in to the appropriate equations of motion, in this case equations 9a and 9c. This yields:

$$\rho \frac{\partial}{\partial x}\left(\frac{\partial^2 \Phi}{\partial t^2}\right) + \rho \frac{\partial}{\partial z}\left(\frac{\partial^2 \Psi}{\partial t^2}\right) = (\lambda + 2G)\frac{\partial}{\partial x}(\nabla^2 \Phi) + G\frac{\partial}{\partial z}(\nabla^2 \Psi) \tag{21}$$

and

$$\rho\frac{\partial}{\partial z}\left(\frac{\partial^2\Phi}{\partial t^2}\right)-\rho\frac{\partial}{\partial x}\left(\frac{\partial^2\Psi}{\partial t^2}\right)=(\lambda+2G)\frac{\partial}{\partial z}(\nabla^2\Phi)-G\frac{\partial}{\partial x}(\nabla^2\Psi) \tag{22}$$

Equations 21 and 22 are satisfied if:

$$\frac{\partial^2\Phi}{\partial t^2}=\frac{\lambda+2G}{\rho}\nabla^2\Phi=\nu_p^2\nabla^2\Phi \tag{23}$$

and

$$\frac{\partial^2\Psi}{\partial t^2}=\frac{G}{\rho}\nabla^2\Psi=\nu_s^2\nabla^2\Psi \tag{24}$$

Using Eulers formula for a sinusoidal wave travelling through a medium in the x-direction, the potential expressions Φ and Ψ can be rewritten:

$$\Phi=\mathbf{F}(z)exp[i(\omega t-Nx)] \tag{25}$$

and

$$\Psi=\mathbf{G}(z)exp[i(\omega t-Nx)] \tag{26}$$

The new functions 25 and 26 describe the change in amplitude of the wave as a function of depth. N is defined as the wave number:

$$N=\frac{2\pi}{L} \tag{27}$$

Where L is the wavelength.
The potential expressions Φ and Ψ can then be substituted into equations 23 and 24, and then rearranged, to yield:

$$\mathbf{F}''(z)-\left(N^2-\frac{\omega^2}{\nu_p^2}\right)\mathbf{F}(z)=0 \tag{28}$$

and

$$\mathbf{G}''(z)-\left(N^2-\frac{\omega^2}{\nu_s^2}\right)\mathbf{G}(z)=0 \tag{29}$$

Where $\mathbf{F}''(z)$ and $\mathbf{G}''(z)$ are derivatives with respect to z. Simplifying further using the relation:

$$q^2=\left(N^2-\frac{\omega^2}{\nu_p^2}\right)\mathbf{F}(z)=0 \qquad\qquad s^2=\left(N^2-\frac{\omega^2}{\nu_s^2}\right)\mathbf{F}(z)=0 \tag{30}$$

Yields the following:

$$\mathbf{F}''(z)-q^2\mathbf{F}(z)=0 \tag{31a}$$

$$\mathbf{G}''(z)-s^2\mathbf{G}(z)=0 \tag{31b}$$

This can then be expanded to the form:

$$\mathbf{F}(z) = A_1 exp(-qz) + B_1 exp(qz) \tag{32a}$$
$$\mathbf{G}(z) = A_2 exp(-sz) + B_2 exp(sz) \tag{32b}$$

To prevent the amplitude of the wave becoming infinite with depth, the condition $B_1 = B_2$ is introduced. This term can then be substituted back into the original potential equations 25 and 26 to yield:

$$\Phi = A_1 exp[-qz + i(\omega t - Nx)] \tag{33}$$
$$\Psi = A_2 exp[-sz + i(\omega t - Nx)] \tag{34}$$

It is then necessary to impose the boundary condition along the surface, in order to differentiate from the rest of the half space. This is the condition of no stresses along the surface (both shear and normal stress), which can be expressed as:

$$\sigma_z = \lambda\overline{\epsilon} + 2G\epsilon_Z = \lambda\overline{\epsilon} + 2G\frac{\partial w}{\partial z} = 0 \tag{35}$$
$$\tau_{zx} = G\gamma_{zx} = G\left(\frac{\partial w}{\partial x} + \frac{\partial u}{\partial z}\right) = 0 \tag{36}$$

By inserting the definitions of u and w into the expanded potential equations, the boundary conditions can be expressed as:

$$\sigma_{z|z=0} = A_1[(\lambda + 2G)q^2 - \lambda N^2] - 2iA_2GNs = 0 \tag{37}$$
$$\tau_{zx|z=0} = 2iA_1NQ + A_2(s^2 + N^2) = 0 \tag{38}$$

Through rearranging, adding, cross multiplying and squaring both sides of this set of equations, one yields the following expression:

$$16G^2N^4\left(N^2 - \frac{\omega^2}{\nu_p^2}\right)\left(N^2 - \frac{\omega^2}{\nu_s^2}\right) = \left[(\lambda + 2G)\left(N^2 - \frac{\omega^2}{\nu_p^2}\right) - \lambda N^2\right]^2\left[N^2 + \left(N^2 - \frac{\omega^2}{\nu_s^2}\right)\right]^2 \tag{39}$$

Which can be simplified by dividing by G^2N^8, and simplified further by applying the following relationships:

$$\frac{\omega^2}{\nu_p^2N^2} = \alpha^2K^2 \tag{40}$$
$$\frac{\omega^2}{\nu_s^2N^2} = K^2 \tag{41}$$
$$\frac{\lambda + 2G}{G} = \frac{1}{\alpha^2} \tag{42}$$

Which, after expansion and rearrangement yields:

$$K^6 - 8K^4 + (24 - 16\alpha^2)K^2 + 16(\alpha^2 - 1) = 0 \tag{43}$$

Equation 43 can be seen as a cubic equation in K^2 with real values given for values of ν, where K represents a *ratio between the velocity of the surface and shear wave.* K^2 is therefore independent of frequency, which means that the velocity of the surface wave is also independent of frequency and is non dispersive. The wave velocities of surface and body waves are all dependent on the Poisson's ratio of the material, and so are all related through this ratio. It can be seen in figure 4 that in materials with a lower Poisson's ratio the wave speeds for all wave types will be similar, whereas in materials with a high Poisson's ratio the wave speed for P-waves increases rapidly compared to the S wave. It should be noted that the wave speeds are all normalized to the S wave speed in figure 4.

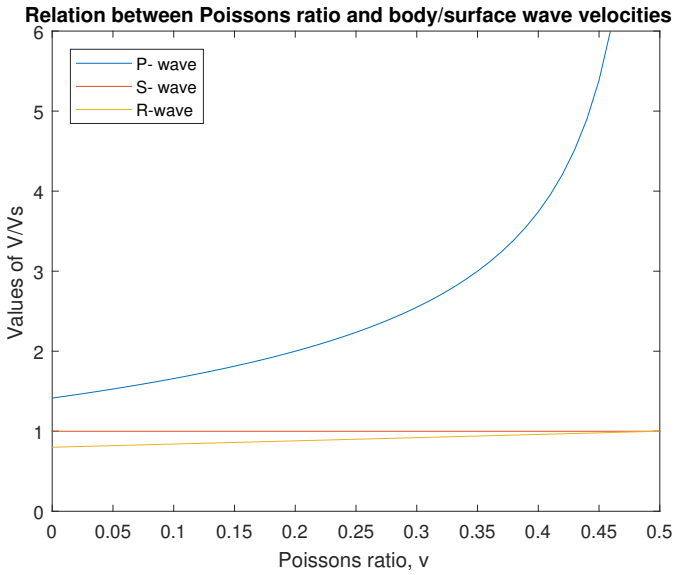

Figure 4: Relation between Poisson's ratio, v, and velocities of compression (P), shear (S) and Rayleigh (R) waves in a semi-infinite elastic medium.[2]

Additional information about the displacement of the Rayleigh wave can be derived by expressing u and w in terms of known quantities. The amplitude of both the horizontal and vertical displacements of the Rayleigh wave are dependent on the depth of the half space and the Poisson's ratio of the material. This can be seen in figure 5.

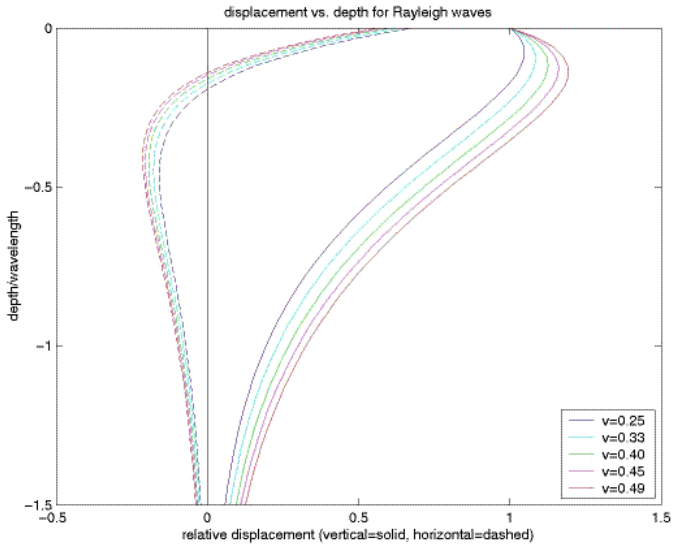

Figure 5: Amplitude ratio vs. dimensionless depth for Rayleigh wave.[7]

Since the discussed wave types all have different propagation velocities, which can be predicted if the material is known, the order in which they arrive at a target can also be predicted with relative ease.
If the surface is excited with a short impulse, a symmetrical annular wave system will propagate away from the point of excitation. The wave system will then consist of the three discussed wave types; P- and S-waves below the surface and Rayleigh waves which propagate along the surface, all at different velocities. The first wave to arrive at the target (at a fixed distance from the point of excitation) is the P-wave, followed by a period of no oscillations, and then the arrival of the S-wave. This is normally referred to as a *minor tremor*, as the next oscillation caused by the Rayleigh wave is of a much larger magnitude and is referred to as a *major tremor*. This can also be clearly seen in figure 4, where the P wave has the highest velocity and the Rayleigh wave has the lowest.

2.2 Elastic waves in layered systems

When a body wave (P- or S-wave) in an elastic medium encounters the interface with another elastic medium, some energy is reflected back into the first medium and some energy is transmitted into the second medium, in accordance with Zoeppritz theory of elasticity [2]. There is a difference between how P- and S-waves interact with interfaces. S-waves are split into two components at an interface;

- SV-waves; which have a motion in a plane perpendicular to the plane of the interface.
- SH-waves; which have a motion in a plane parallel to the interface.

An illustration of the interaction of body waves at an interface between two elastic media has been shown in figure 6.

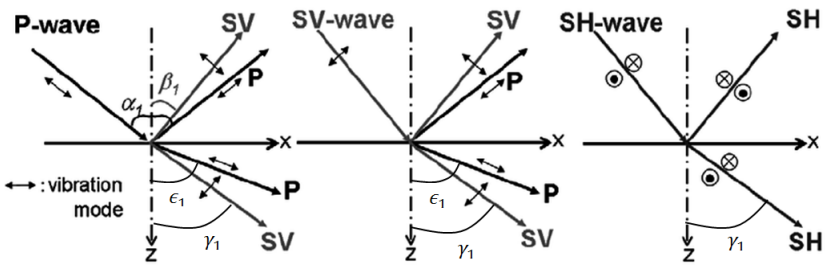

Figure 6: Partition of elastic waves at interface between two elastic media.[8]

It can be seen that P-waves can induce SV-waves, both as a reflective wave back into medium one, and as a transmissional wave into medium two. This is reciprocal for SV-waves, which induce P-waves, both as reflective and transmissive waves into medium one and two respectively. SH-waves, however, only give rise to other SH-waves, both as reflective waves into medium one and transmissive waves into medium two.
The exit angle of the reflected or transmitted wave depends on the angle of incidence and the ratio of wave velocities between the two media, and can be seen in figure 6. Snell's law can therefore be used to find all of the exit angles.

$$\frac{sin\alpha_1}{\nu_{P1}} = \frac{sin\beta_1}{\nu_{S1}} = \frac{sin\epsilon_1}{\nu_{P2}} = \frac{sin\gamma_1}{\nu_{S2}} \tag{44}$$

Where α_1, β_1, ϵ_1 and γ_1 are angles normal to the interface and:

- ν_{P1} is the velocity of the P-wave in medium one.
- ν_{S1} is the velocity of the S-wave in medium one.
- ν_{P2} is the velocity of the P-wave in medium two.
- ν_{S2} is the velocity of the S-wave in medium two.

The amplitude of the resulting waves are also a function the angle of incidence of the incident wave and the ratio of velocities between the two media. An interesting result of this relationship is that if the material properties, and therefore wave propagation velocities, are known, then the amplitude of the resulting waves is only dependent on the angle of incidence. It is therefore possible to calculate the relative amplitude of the resulting waves over all possible incident angles (0-90°), finding the maximum and minimum amplitudes as a function of angle of incidence.

2.2.1 Rayleigh waves in a vertically layered system

As Rayleigh waves propagate along the surface of an elastic half space, the wave types discussed in section 2.2 are not applicable when considering Rayleigh waves. If discontinuities occur along the surface of the half space, and the incoming Rayleigh wave encounters an interface between two media of different density (and therefore propagation velocity), it is interesting to determine the mechanism that will transpire.
At a vertical interface, the energy from the incident Rayleigh wave is divided into three wave types:

- A reflected Rayleigh wave.
- A transmitted Rayleigh wave.
- Reflected body waves.

The energy distribution between these wave types is dependent on the corner angle and Poisson's ratio. An illustration of the Rayleigh wave-interface interraction can be seen in figure 7.

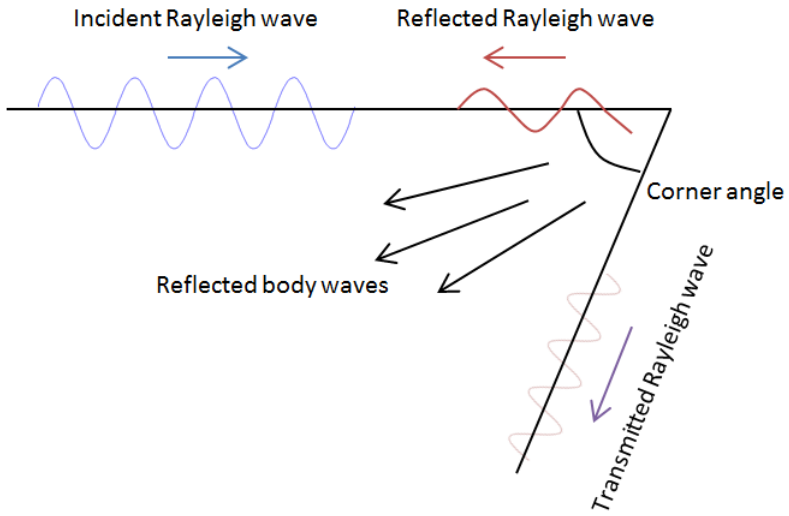

Figure 7: Partition of Rayleigh wave energy at a corner.[2]

2.2.2 Love waves and head waves

When a reflected wave returns to the surface of a layered elastic half space, it encounters the interface between the solid and void. This large change in impedance will lead to total reflection. A second type of surface wave, known as a **Love wave**, can occur is many total reflections occur. A Love wave is a horizontally polarised shear wave which acts in a superficial layer and which is propagated by numerous total reflections. This motion can be seen in figure 8.

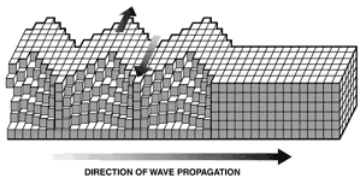

Figure 8: The motion of Love waves in a layered elastic half space. [6]

It should be noted that Love waves do not occur if the top layer has a higher velocity than the bottom layer. Love waves have a propagation velocity between that of the shear wave velocity in the superficial layer and the shear wave velocity in the layer below.
Head waves are the name given to P-waves that have been caused by a wave travelling along the interface plane, thereby causing another wave to be refracted back to the surface.

2.2.3 Wave attenuation

As a wave travels through a medium, or meets an intersection between two media, absorption occurs. This is a process of transforming the mechanical energy of the wave into heat, which in turn reduces the amplitude of the wave. The process is also known as damping. In geodynamics two types of damping are important:

- **Material damping**. This is also known as inner damping and is most dependent on the materials shear modulus. But other geotechnical variables such as moisture content also has an affect on the inner damping of the material.
- **Geometrical damping**. This process describes how the different wave types amplitude decreases with distance from the source. As surface waves propagate outwards in a circle, the reduction of the amplitude can be calculated with $\frac{1}{r^{\frac{1}{2}}}$, whereas body waves propagate outwards in a half sphere, so the amplitude reduction would be equivalent to $\frac{1}{r}$. [9]

A combination of material damping and geometrical damping can be used to find the amplitude of a wave in a large volume of homogeneous material, using the following equation:

$$A_2 = A_1 \left(\frac{R_1}{R_2} \right)^n e^{-\alpha(R_1 - R_2)} \tag{45}$$

Where A_1 and A_2 are the amplitudes at the respective distances R_1 and R_2, the factor n is used to describe the wave form, where $n = 1$ for body waves in a sphere, $n = 2$ for body waves along the surface of a half-sphere and $n = \frac{1}{2}$ for surface waves. The coefficient α is the absorption coefficient in the material [9]. It should also be noted that although there is a progressive non-linear reduction in wave amplitude due to material damping, these losses are small compared to geometrical damping [5] for softer materials being exposed to a point-excitation.

2.3 Vibration isolation

There are three approaches to isolating a structure from ground vibrations. [10]

- **Restrictions at the source of vibrations**. This method varies depending on the source. To reduce the amplitude of ground vibrations from a road, the traffic speed can be reduced. If the source is a machine, the operating frequency can be modified or the dynamic response of the machines foundations can be improved. Passive isolation involves moving the source further from buildings where people live or work. The use of existing geological formations, such as sound, deep seated bedrock, will experience smaller vibration amplitudes than foundations on soil or other weather materials. [2]
- **Screening of the waves propagating through the soil**. This involves the installation or construction of barriers underground. This concept is based on reflection, scattering and

diffusion of wave energy. Known barriers are slurry filled trenches, sheet piles or concrete walls. There are some general guidelines to observe when positioning any barriers underground. If the source and receiver positions are known, the barrier should ideally be placed as close as possible to the source or the receiver, but not half way in between, as refraction around the bottom of the barrier could lead to an increase in the velocity levels at the receiver location [11].

- **Isolation of the structure being affected by ground vibrations**. If the vibration levels are too high, and the above approaches can not be used, there are well established methods which can be used to isolate structures from ground vibrations. The most common method is the use of seismic mountings. Although there are other, more exotic methods used in areas of high earthquake activity.

Increasing the stiffness, and therefore the natural frequency of the ground can also be an effective means at reducing the velocity levels of ground vibrations. This is normally done if the excitation is a constant low frequency excitation, such as from a machine, which could match or be close to the natural frequency of the ground. It is therefore desirable to have a higher natural frequency in the foundation than the excitation source in order to achieve more damping. The stiffness of the ground can be achieved through chemical means or by mixing cement into the ground [12].

3 Method

To gauge the effectiveness of different wave barriers in different ground types, finite element modelling (FEM) was performed in the solid mechanics module of the program COMSOL^{TM}multiphysics. The results of these simulations were then processed in MATLAB^{TM}to model the reduction of the velocity levels over distance and frequency. FEM was used for this task for the following reasons:

- Complex and powerful tool for solving engineering problems.
- COMSOL^{TM}uses a simple user interface and layout, simplifying the simulation process.
- Gives accurate results even at low frequencies. Other modelling tools such as Statistical Energy Analysis (SEA) only give accurate results at considerably higher frequencies than considered here.
- FEM can be used for complex geometries.

3.1 Modelling of a section of ground

In order to properly simulate the propagation of different wave types through different ground types, the geometry and size of the 3D space had to be chosen carefully. The following had to be considered when choosing the geometry:

- Large size to allow the propagation of the low frequencies (large wavelength) in the model. But not too large that the simulation times become too long.
- A favourable geometry in order to see the Rayleigh waves on the surface and the body waves underground.

Using the above considerations, it was deemed appropriate that a $\frac{1}{4}$ sphere, with a radius of 30 meters be used.

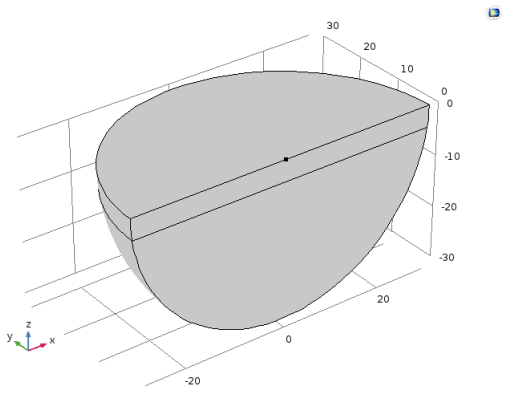

Figure 9: Geometry of the model.

The boundary conditions for this model had to be selected carefully to give accurate simulations. The boundary conditions given were as follows.

- The $x-y$ plane was chosen to represent the surface layer, so was given the boundary condition *free layer*. This means that there are no constraints and no loads acting on the boundary [13]. This is important for the propagation of surface waves as discussed in section 2, as it creates the needed half space with the free layer.
- The *point load* was placed at origo in order to get a symmetrical wave propagation in all directions. The load was modelled as an impulse.
- The boundary condition *low-reflecting-boundary* was given to the outside surface of the $\frac{1}{4}$ sphere in order to eliminate any reflections. As a default, it takes material data from the domain in an attempt to create a perfect impedance match for both pressure waves and shear waves. It can be sensitive to the direction of the incoming wave [13]. This can be a problem as it takes the average wave speed between the P- and S-waves, which for this type of problem vary greatly.
- The $x-z$ plane was given the *symmetry* boundary condition.

The mesh size should, when dealing with any acoustic model, be far smaller than the considered wavelengths, so that no information is lost. While this can be a problem for simulating high frequency phenomena, as a small mesh size would need to be used in order to capture all desired wavelengths, this was not a particularly large issue in this case, as the highest studied frequency, 50Hz, had a wavelength for S-waves of over 1m for the softest ground type, as shown in figure 10. This means that a relatively large mesh size could be used which lowered the calculation time significantly. The standard element shape, the tetrahedron, was used exclusively in this model, as it required little input from the user and is ideal for modelling the spherical shape with ease. The equations being solved are the differential equations for the equations of motion (equation 4) in an elastic half space, as shown in section 2. The different boundary conditions for different cases were also discussed in section 2, with the surface layer elements possessing other boundary conditions compared to the elements which are below the surface layer. The analytical solutions to these equations for these different cases are shown in some detail in section 2.
The absolute velocity levels in the Z-direction were then taken along a vector, starting at the *point load* position and ending at the outer boundary of the sphere, making the total vector length 30m. The vector position was made to cross over any barrier, and if any information was deemed missing or any phenomena was observed in the results that was unclear, a reverse Fourier transform was performed and the simulation was performed in the time domain in order to see observe different physical phenomena more clearly. This method worked well for all boundary types where the geometry was symmetrical over the entire boundary span, but for one boundary type a different method was used.

3.2 Ground and barrier types

In order to determine the effectiveness of different barriers, it was necessary to choose three ground types which would represent a good average of the ground types encountered, in relation to density, bulk- and shear modulus and Poisson's ratio. This was also important since the wave speed is dependent on the bulk modulus and density of the material, as discussed in section 2. The appropriate material properties for the studied ground types can be seen in table 1. The wavelengths for frequencies up for 50Hz can be seen in figure 10.

Ground type	Density kg/m^3	Poisson's ratio	E-modulus N/m	P-wave speed m/s	S-wave speed m/s	Loss factor
Soft, sandy soil	1600	0.49	$63.7 \cdot 10^6$	1400	115	0.1
Clay	2125	0.48	$340 \cdot 10^6$	2000	232	0.1
Bedrock	2600	0.4	$8809 \cdot 10^6$	4159	1100	0.04

Table 1: The densities, Poisson's ratios, bulk moduli, body wave velocities and loss factors for the studied ground types.

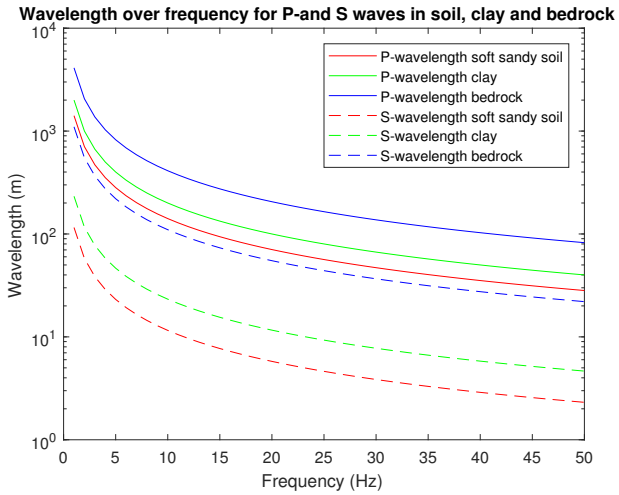

Figure 10: S-and P wavelengths in all ground types up to 50Hz.

A number of different barrier types were studied, in order to try and see which parameter; cylinder size or center-center distance, had the largest effect on the velocity levels of low frequency ground vibrations. The orientation of these barrier types can be seen in figure 11 below.

- Barrier 1: A trench, 6m deep and 0.5m wide.
- Barrier 2: Single row of cylinders, 15cm radius and 1m center-center distance.
- Barrier 3: Single row of cylinders, 30cm radius and 1m center-center distance
- Barrier 4: Single row of cylinders, 15cm radius and 0.5m center-center distance.
- Barrier 5: Single row of cylinders, 30cm radius and 0.8m center-center distance.
- Barrier 6: Double row of cylinders, 15cm radius and 1m center-center distance.
- Barrier 7: Four rows of cylinders, 15cm radius and 1m center-center distance.
- Barrier 8: Cylinders in a circular pattern, holes with 15cm radius, circle radius 3m and segment angle 32.7°.

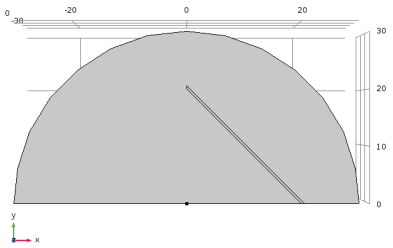

(a) A trench, 6m deep and 0.5m wide.

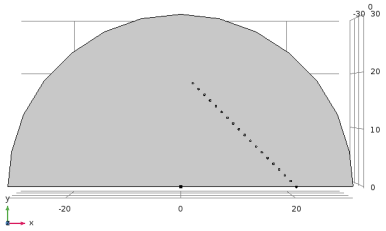

(b) Single row of cylinders, depth 9m,15cm radius and 1m center-center distance.

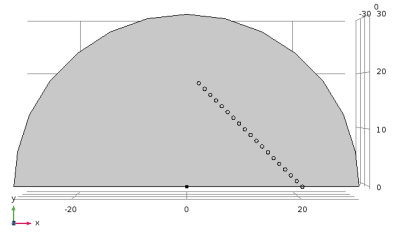

(c) Single row of cylinders, depth 9m, 30cm radius and 1m center-center distance.

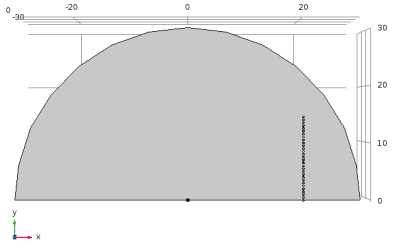

(d) Single row of cylinders, depth 9m, 15cm radius and 0.5m center-center distance.

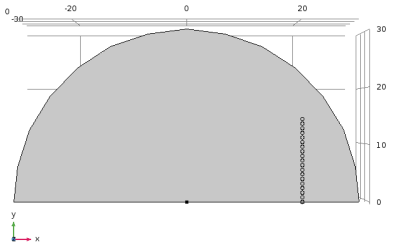

(e) Single row of cylinders, depth 9m, 30cm radius and 0.8m center-center distance.

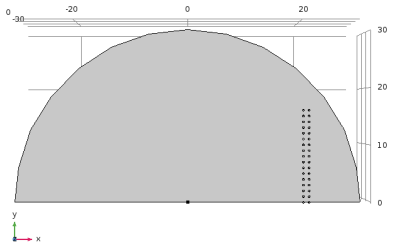

(f) Double row of cylinders, depth 9m, 15cm radius and 1m center-center distance.

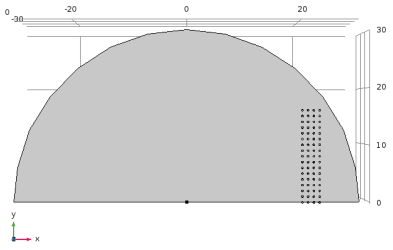

(g) Four rows of cylinders, depth 9m, 15cm radius and 1m center-center distance.

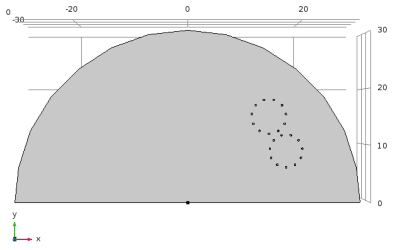

(h) Circular pattern radius 3m, holes 15cm radius, depth 9m, segment angle 32.7°.

Figure 11: Types and orientations of different barriers.

The barriers were placed 20m from the point of excitation to allow for the attenuation of the higher frequencies which can be present close to the excitation. The velocity levels were then extracted along a vector from the source to the edge of the domain, in order to see the difference in velocity levels immediately before and after the barrier. A 6m deep, 0 5m wide trench was simulated, partly to validate the model and partly to have a bench mark for the other barrier types, as a trench is an extremely effective way of dampening all incoming frequencies.
It should be noted that the cylinders were modelled to be containing *air*, which has a density of $1.225\frac{kg}{m^3}$, no Poisson's ratio, a bulk modulus of 101kPa, a P-wave speed of $342m/s$ and no S-wave speed.

4 Results

4.1 Simulation results

As the $X-Y$ plane is the free surface plane of the model, it is most appropriate to extract the velocity levels in the Z dimension, as most of the energy is in the surface wave, as discussed in section 2, and the movement of the Rayleigh wave is elliptical, with a larger Z-component. It should be noted that while the Z-component is most prominent at shorter distances, at larger distances ($> 500m$) the X-component of the ellipse can become greater than the Z-component depending on the ground type [11]. The reduction of velocity levels was done by taking the difference between the velocity without any barrier and the velocity level when one of the barrier types mentioned in section 3.2.

In order to gauge the effectiveness of any barrier, the velocity levels for each frequency needed to be plotted over distance from the excitation point source when no barrier is present.

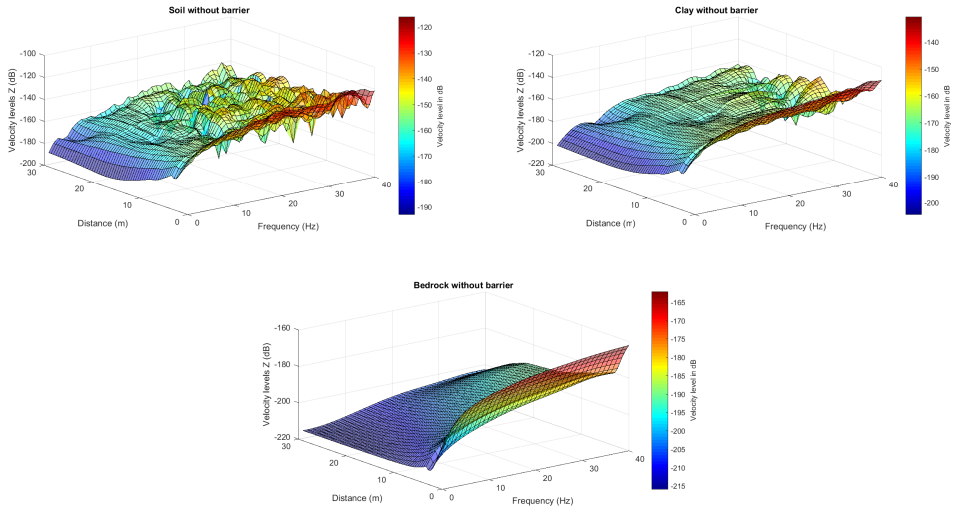

Figure 12: Velocity levels along the radius of the quarter sphere across the entire frequency band for three ground types **without any barrier**. The upper left figure is for soft, sandy soil. The upper right figure is for clay and the bottom figure is for bedrock.

It is clear that the materials with a smaller bulk modulus give rise to a more chaotic interference pattern created by the three different wave types even at shorter distances, since the wave lengths, particularly for the shear waves are far shorter, as seen in figure 10. It can be seen that as the frequency increases the amount of interference also increases in clay and soil. Bedrock has a very high density and stiffness which give very high wave speeds and large wave lengths for P- and S-waves as seen in table 1 and figure 10, and given the limited size of the geometry no interference can be observed on the surface at these low frequencies. It should be noted that it is mostly the Rayleigh wave that produces any surface velocities in the Z-direction, but the S-wave's propagation

and motion also produces a displacement at the surface in the Z-direction. Figure 12 also shows the expected effect of geometrical damping, showing a clear decrease over distance.

The next step in these simulations was to compare the velocity levels with the different kinds of barriers against those shown in figure 12. This was achieved simply by taking the difference in the results matrices for the different barriers in the different ground types against the matrix for the results without a barrier. It was then possible to see which barrier types had the greatest effect on different frequencies.

4.1.1 A 6m by 0.5m trench

In order to verify that the FEM model worked, and that all of the boundary conditions were correct, it was deemed necessary to try and model a simple trench. In reality any large volume which gives a large impedance change could be used to test the model, but in this case a large air gap was used. Such methods are already in use and have a well documented effect on reducing the velocity levels of ground vibrations [2]. The velocity levels for frequencies between $1 - 40$Hz over a distance of 30m can be seen in figure 13 where the trench position is at 20m.

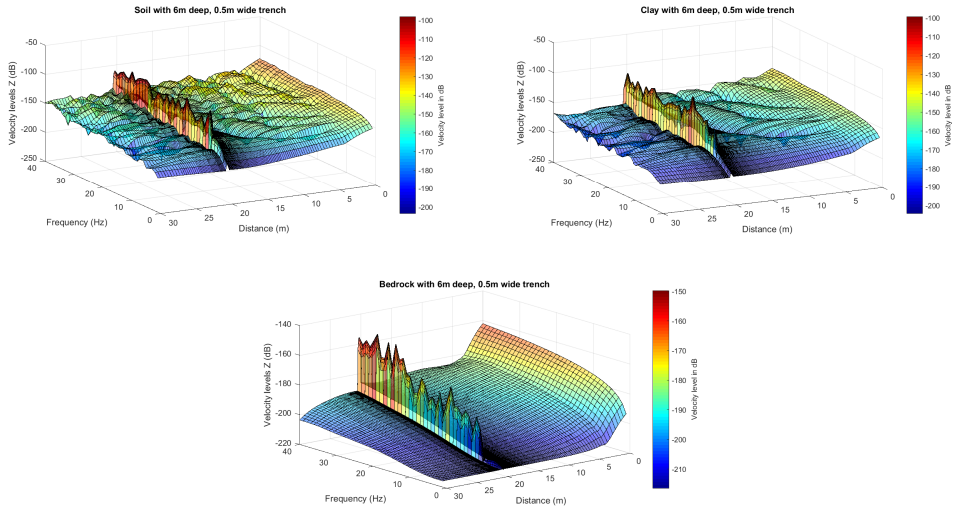

Figure 13: Velocity levels along the radius of the quarter sphere across the entire frequency band for three ground types **with a trench**. The upper left figure is for soft, sandy soil. The upper right figure is for clay and the bottom figure is for bedrock.

There is a clear drop in velocity level after 20m, which is the position of the trench. The large increase in velocity level at the trench position is because the air gap is compressed by the incoming body waves which causes a large increase in the velocity of the air, giving the large peak. There is also a relatively large peak before the trench position compared to figure 12. This is because there is a large reflection at the barrier which constructively interferes with incoming waves to give a peak in the velocity levels immediately before the trench. This area of interference is larger for the

lower frequencies as the wave lengths involved are longer. In order to see these effects more clearly, the $Y - Z$ view has been presented in figure 14.

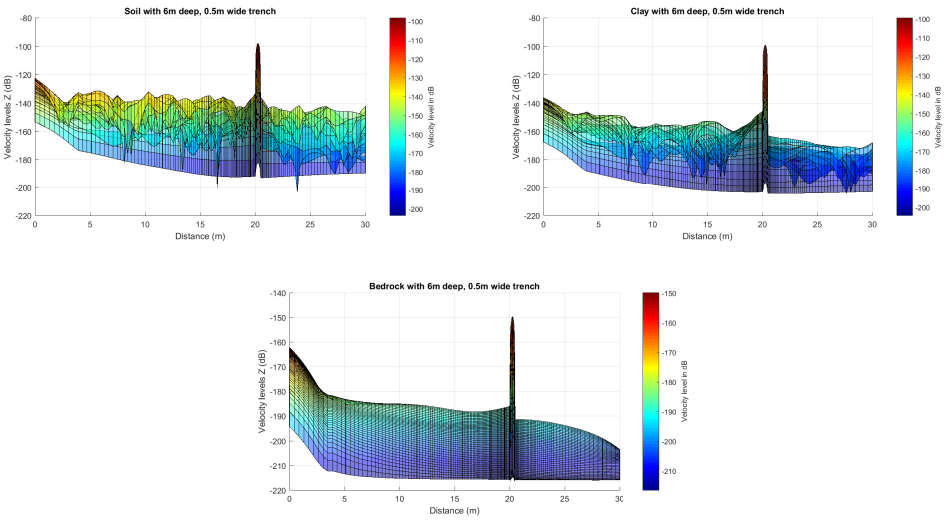

Figure 14: Velocity levels along the radius of the quarter sphere across the entire frequency band for three ground types **with a trench**. The upper left figure is for soft, sandy soil. The upper right figure is for clay and the bottom figure is for bedrock. Here observed in the $X - Y$ perspective.

The most important result is the difference in velocity levels between figures 12 and 13. As the trench is of sufficient dimensions to give a significant reflection of the waves at all incoming frequencies there should be a reduction across the entire frequency band. The only area of interest is also after the trench position, so all results up to 21m have not been shown in the following figure.

It is clear that there is a clear reduction for all ground types after the trench position, but the interference pattern created by the three different waves in the softer ground types makes the results harder to interpret for individual frequencies from the view in figure 15. The results indicate that the lower frequencies ($f < 10Hz$) are difficult to damp with a trench, and this seems to be true regardless of the ground type. This could be because the longer wavelengths do not travel enough distance around the trench to be sufficiently damped, and could be solved by having a trench with larger dimensions to allow for more geometrical damping. The increase in velocity levels at the lower frequencies in the softer ground types could be caused by constructive interference by refraction and a phase shift of the surface wave as it changes direction at the corner of the trench. The middle frequencies ($10Hz > f < 30Hz$) are affected by the trench quite significantly, having the velocity level reduced by up to 30dB in certain positions after the trench. In the higher frequencies ($f > 30Hz$) there is an immediate increase in the velocity levels for all ground types, but given then erratic nature of these peaks and dips it is most likely due to a superposition of different body waves, as well as an acute refraction angle at the bottom of the trench, causing this phenomena to occur. There is also the possibility that the *low-reflecting-boundary* does reflect certain frequencies more than others, as the difference in wave speed between the pressure and shear waves in difference ground types (see table 1) gives an average wave speed which differs greatly from the actual wave

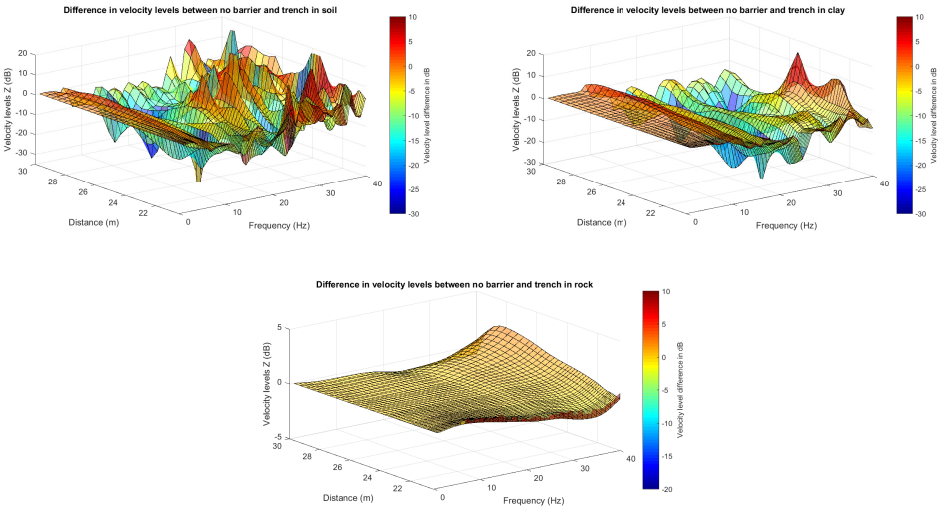

Figure 15: Velocity level difference between three ground types over distance and frequency with and without a trench. The upper left figure is for soft, sandy soil. The upper right figure is for clay and the bottom figure is for bedrock.

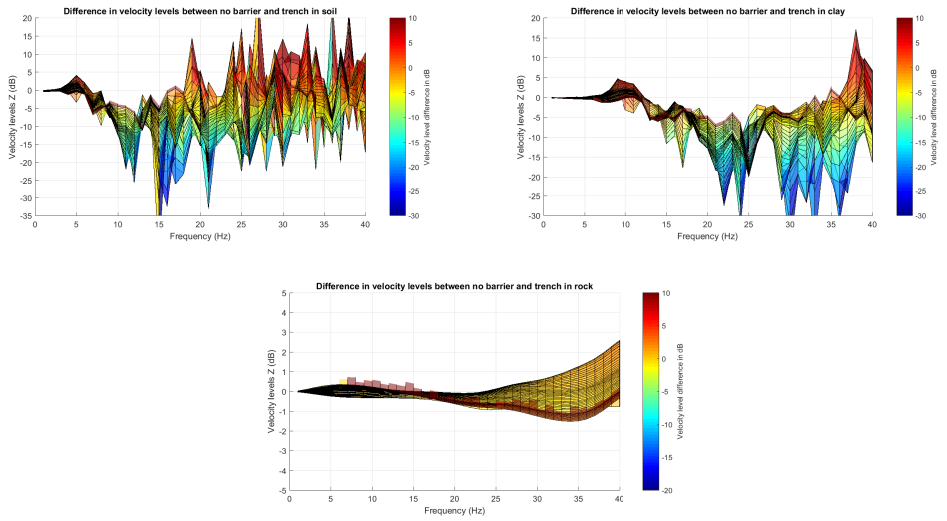

Figure 16: Velocity level difference between the softer ground types over distance and frequency with and without a trench seen in the $X - Z$ perspective. The left figure is for soft, sandy soil and the right figure is for clay.

speeds, causing small amounts of reflection to occur. This would most likely only effect the low frequencies in this model.

Since the interference pattern of the softer ground types makes figure 15 difficult to interpret, the $X - Y$ view with the colour scale has been shown in figure 17 to allow for easier interpretation.

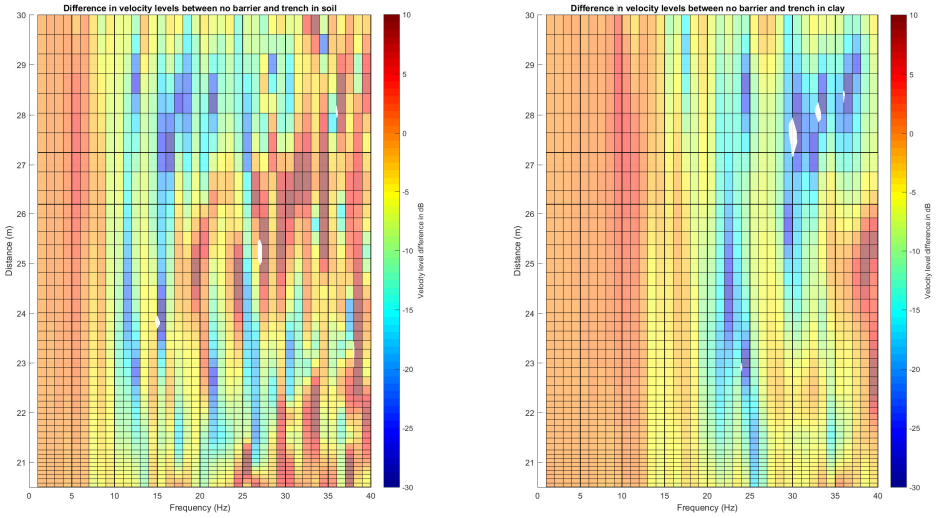

Figure 17: Velocity level difference between the softer ground types over distance and frequency with and without a trench seen in the $X - Y$ perspective. The left figure is for soft, sandy soil and the right figure is for clay.

From figure 17 it is clear that there is a broadband reduction, and the interference pattern is more prominent in the softest material, which is to be expected. Despite some prominent peaks which actually increase the velocity levels for certain frequencies, there is clearly a strong reduction for most frequencies at all distances after the trench. It should be noted that the interference seems to increase with distance from the trench.

In order to confirm that refraction around the bottom of the trench is causing this interference, a reverse Fourier transform was performed on the frequency response function in order to simulate the model in the time domain. The wave front was then observed over time in order to see the behaviour around the bottom of the trench, and refraction was indeed observed, as seen in figure 18.

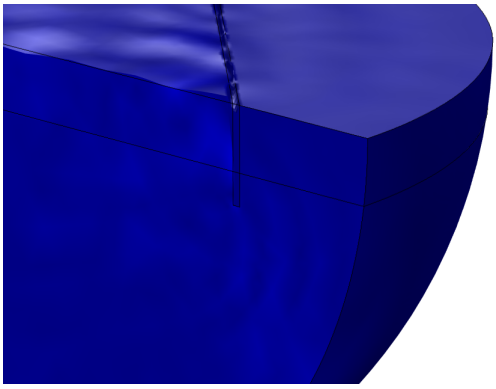

Figure 18: An observation of refraction around the bottom of the trench in the time domain.

The strong reflection of the body waves can also be seen to the lower left of the trench, as well as the interference from the reflections both under- and on the surface immediately before the trench. The deformation of the trench walls can also be seen. This is both from the incoming pressure wave under the surface and from the Rayleigh wave following the trench surface. This acts as a kind of geometrical damping for the Rayleigh wave as distance is therefore being added to the wave path. It can therefore be hypothesized that a trench with increased dimensions would increase the reduction even further for the Rayleigh wave. It is clear, however, that the displacement field in the direction of the wave path is far smaller before and after the trench. The observed results for the trench in both the time and frequency domains indicates that the model works, as the velocity level amplitude before and after the barrier position are very similar to what can be found in other literature [2], where a clear increase is seen before the trench position and a clear drop is shown after the trench position.

4.1.2 Single row of cylinders, 15cm radius and 1m center-center distance.

To begin trying to filter individual frequencies, a single row of cylinders was modelled, and the frequency response function of the model was observed both in the time and frequency domains, and the same procedure as in section 4.1.1 was followed to see the difference in velocity levels for each ground type without any barrier against the velocity levels with the single row of cylinders. The velocity levels for this barrier type can be seen in figure 19.

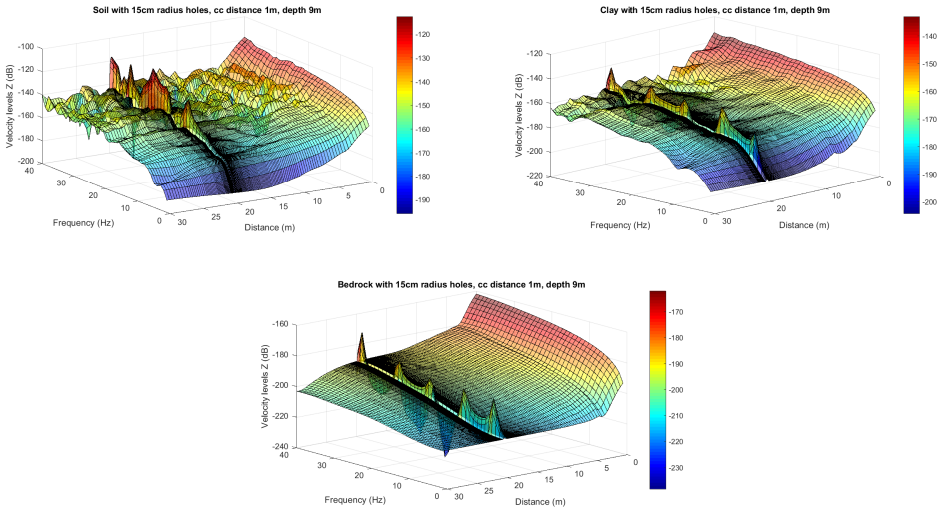

Figure 19: Velocity levels for all ground types over distance and frequency with a **single row of** 15**cm cylinders with a center-center distance of** 1**m**. The upper left figure is for soft, sandy soil. The upper right figure is for clay and the bottom figure is for bedrock.

When comparing the velocity levels for the trench in figure 13 and the single row of cylinders in figure 19 it is clear that the trench is far more effective at reducing the velocity levels of surface waves than the single row of cylinders, as after the barrier position there is a clear drop in velocity levels in figure 13 as compared to figure 19 where there is no apparent reduction in the velocity levels after the barrier position for either ground type. To confirm this observation, the velocity levels after the barrier position were compared with the velocity levels in the ground without any barrier to give the results in figure 20.

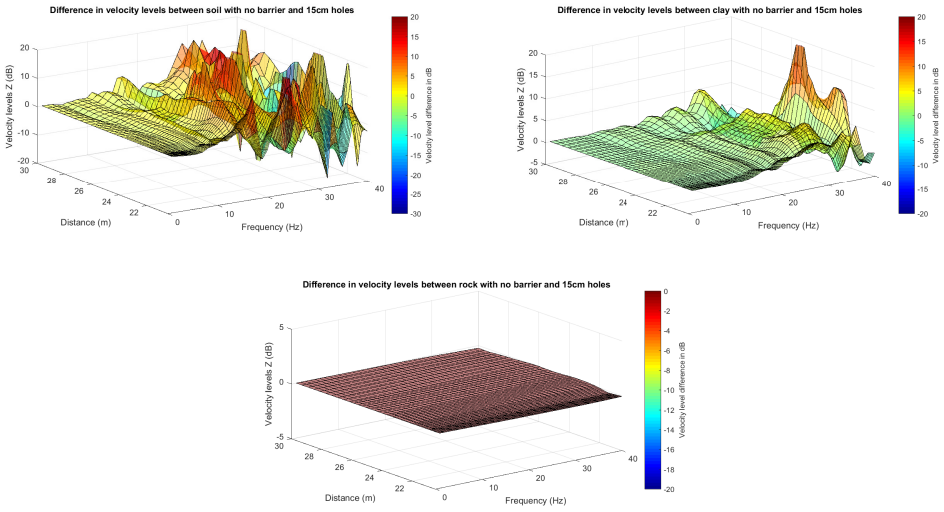

Figure 20: Velocity level difference for all ground types over distance and frequency with a **single row of** 15**cm cylinders with a center-center distance of** 1**m**. The upper left figure is for soft, sandy soil. The upper right figure is for clay and the bottom figure is for bedrock.

Because the interference effects in the softer ground types make figure 20 slightly difficult to interpret, the $X - Y$ perspective has been shown in figure 21. While it is clear that the trench is clearly more effective, there appears to be a filtering of certain frequencies in the softer ground types, but the combination of refraction and scattering at higher frequencies gives rise to both destructive and constructive interference after the barrier position. There also appears to be a greater difference in velocity levels immediately after the barrier (after 20m) which could be caused by the immediate refraction around the edge of the cylinder. This phenomena was observed in the time domain as seen in figures 22(a) through 22(c), where the displacement field becomes clearly more chaotic close to the barrier. It is unclear if there is refraction around the bottom of the cylinders for the body waves, as the small size (relative to wavelength) of the cylinders would most likely not be able to refract any of the frequencies of interest. It should also be noted that there is no significant reduction of the displacement field after the barrier position compared to the trench seen in figure 18.

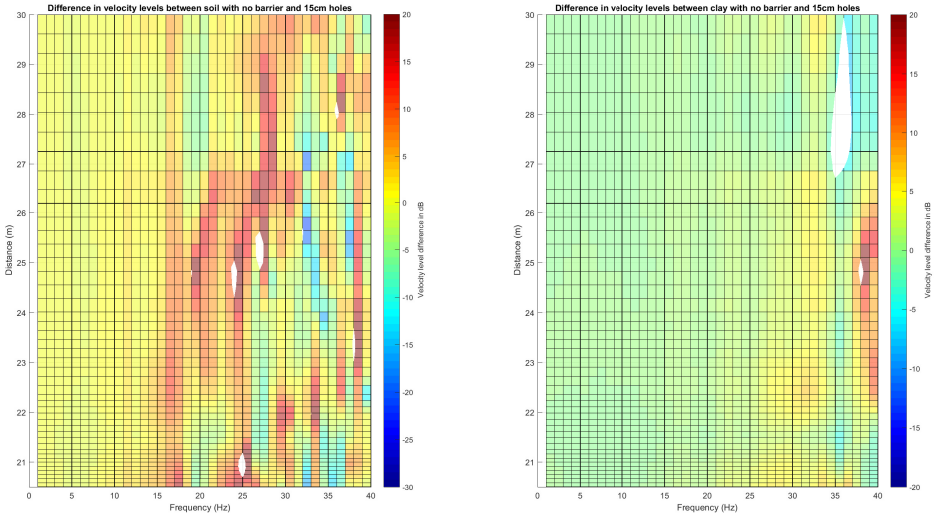

Figure 21: Velocity level difference for softer ground types over distance and frequency with a **single row of** 15**cm cylinders with a center-center distance of** 1**m**. The left figure is for soft, sandy soil and the right figure is for clay.

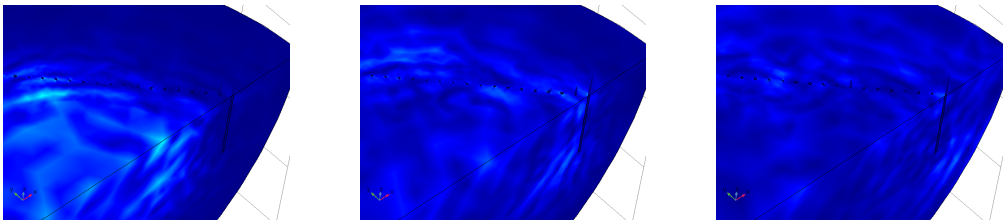

(a) (b) (c)

Figure 22: Time lapse of the wave front hitting the single row of cylinders.

4.1.3 Single row of cylinders, 30cm radius and 1m center-center distance

As part of the parameter study, individual variables were studied to determine if they had an effect of the velocity levels of the surface waves. In order to determine the effect of increasing the radius of the individual cylinders, the cylinder radius was increased to 30cm. The center-center distance of the individual cylinders was not altered from the previous case. The velocity levels between 1 to 50Hz over the entire distance can be seen in figure 23. While the characteristic increase in velocity can be seen at the cylinder position, indicating some degree of absorption, there is no clear reduction after the cylinder position, or even an increase of velocity immediately before the cylinder position, indicating a lack of reflection as well as a lack of reduction. This is an indication that

besides geometrical damping, the only attenuating phenomena to occur at the barrier position are scattering and absorption, whereas for a trench significantly more energy is attenuated through *both reflection and absorption*. It should be noted that scattering can occur in all directions (including back towards the source) and this does reduce the amplitude to an extent, the transfer of energy from the ground to the air in the cylinders would be minimal, which perhaps shows why no significant reduction of the amplitude occurs after the barrier position. The particle velocity could also be increased locally around the cylinder which also could contribute to any reduction, as the loss is proportional to the particle velocity.

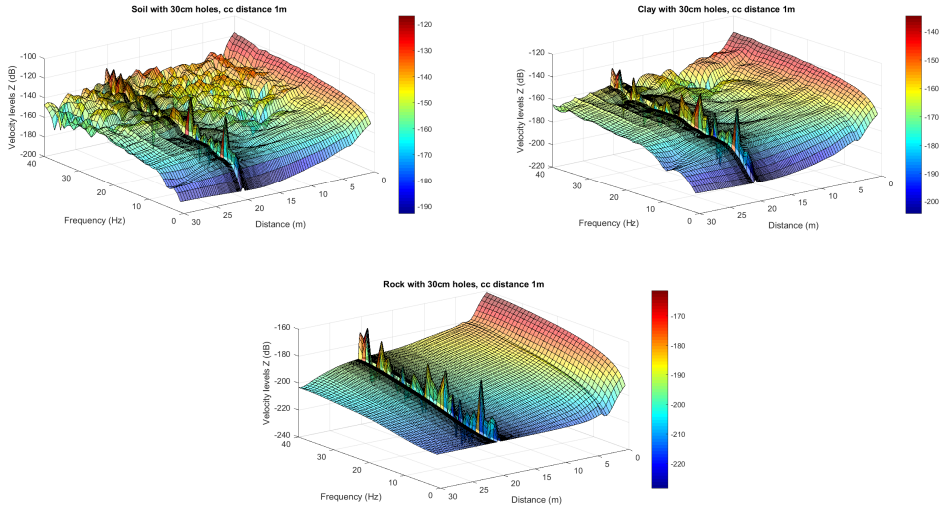

Figure 23: Velocity levels for all ground types over distance and frequency with a **single row of** 30**cm cylinders with a center-center distance of** 1**m**.The upper left figure is for soft, sandy soil. The upper right figure is for clay and the bottom figure is for bedrock.

The difference in velocity levels between figure 23 and 12 after the barrier position can be seen in figure 24. While it is clear that no reduction was achieved for the bedrock, a slight filtering of the higher frequencies seems to occur for clay and soil. It is unclear, however, if this is due to a combination of refraction and scattering around the cylinders than an actual attenuation effect of the cylinder. The $X-Y$ orientation for soil and clay in figure 24 can be seen in figure 25, but this does not serve to help understanding what is causing the variations in velocity level, only where it occurs.

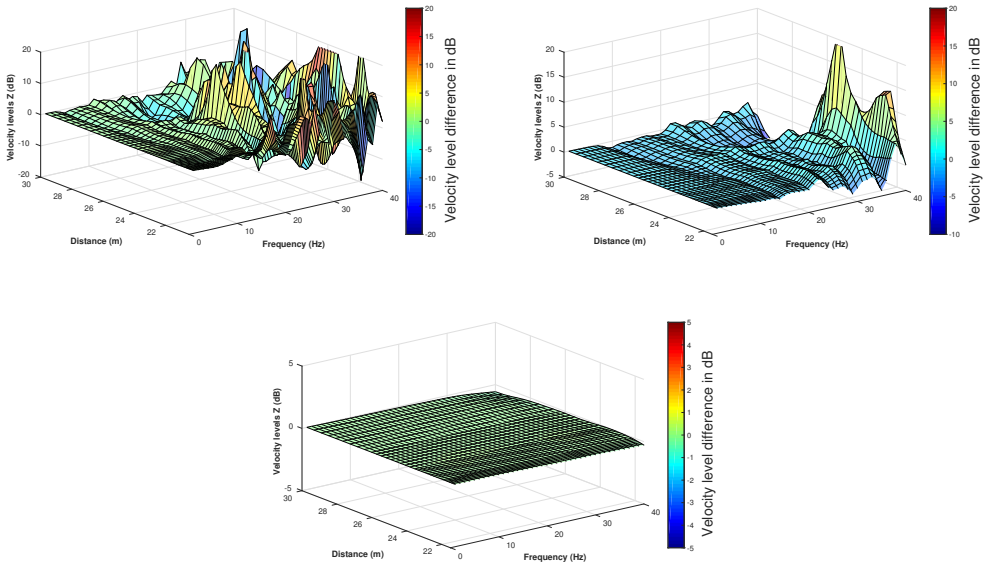

Figure 24: Velocity level difference between all ground types without any barrier and a **single row of** 30**cm cylinders with a center-center distance of** 1**m**.The upper left figure is for soft, sandy soil. The upper right figure is for clay and the bottom figure is for bedrock.

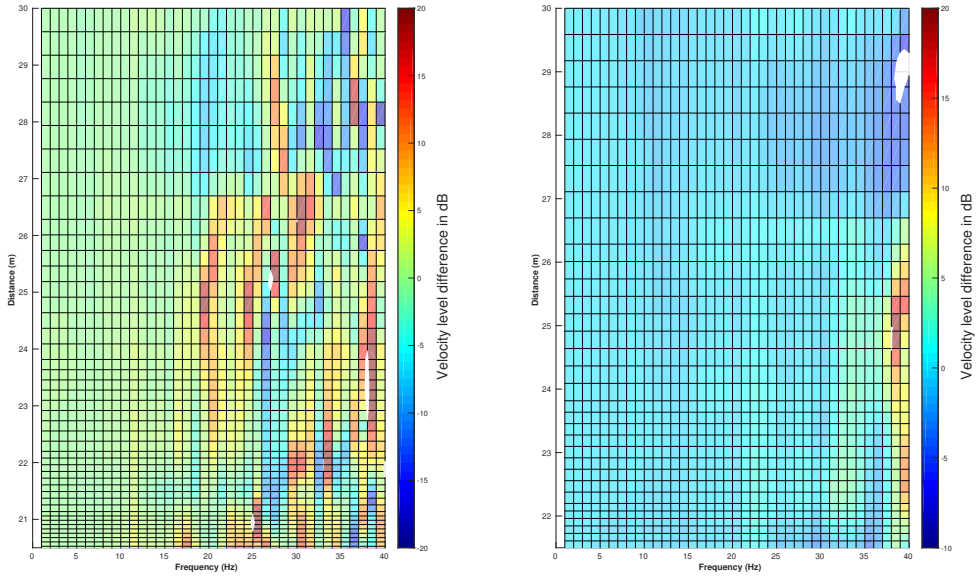

Figure 25: Velocity level difference for softer ground types over distance and frequency with a **single row of** 30**cm cylinders with a center-center distance of** 1**m**.The left figure is for soft, sandy soil and the right figure is for clay.

The average difference in velocity level over all frequencies at all distances after the barrier position does not seem to be to far from zero for either soil or clay, despite there being large local differences down to 20Hz for soil, this seems to be strictly due to the interference pattern occurring at the corresponding wavelengths.

4.1.4 Single row of cylinders, 15cm radius and 0.5m center-center distance

The center-center distance of the hollow cylinders was also thought to have an effect on the propagation of surface waves. To study this, 15cm radius cylinders were placed only 0.5m away from each other, instead of 1m such as in section 4.1.2. An increased reduction was expected relative to a larger center-center distance. The velocity levels between 1 to 50Hz over the entire distance can be seen in figure 26. An increase in velocity can be seen at the cylinder position, which is to be expected. This sharp increase indicates some form of energy transfer and therefore some degree of absorption. There is, however, no clear reduction after the cylinder position for most frequencies, or an increase of velocity before the cylinder position. This could indicate that reflection does not occur to the same extent as with the trench, for example. This is an indication that besides geometrical damping, the only attenuating phenomena to occur at the barrier position are scattering and absorption, whereas for a trench significantly more energy is attenuated through *both reflection and absorption*. It should be noted that scattering can occur in all directions (including back towards the source) and this does reduce the amplitude to an extent, the transfer of energy from the ground to the air in the cylinders would be minimal, which perhaps shows why no significant reduction of

the amplitude occurs after the barrier position. The particle velocity could also be increased locally around the cylinder which also could contribute to any reduction, as the loss is proportional to the particle velocity.

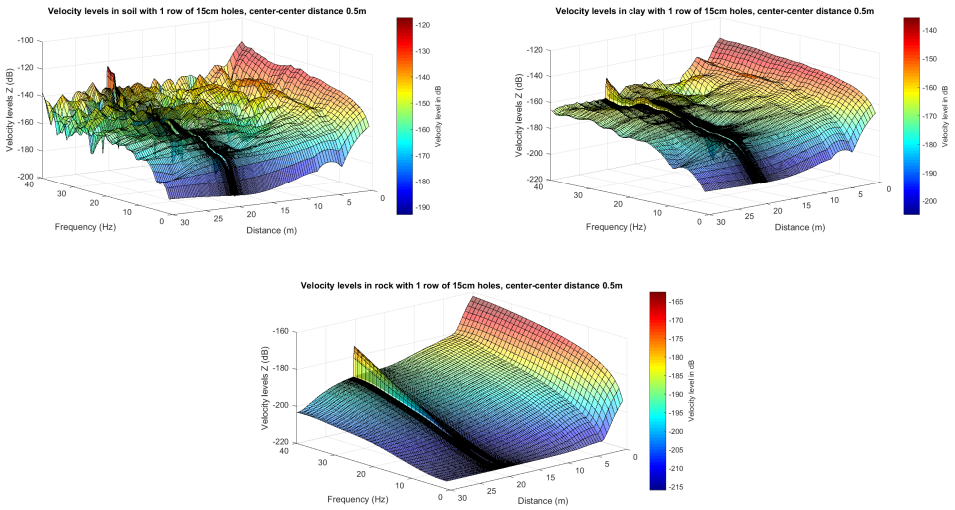

Figure 26: Velocity levels for all ground types over distance and frequency with a **single row of** 15**cm cylinders with a center-center distance of** 0.5**m**. The upper left figure is for soft, sandy soil. The upper right figure is for clay and the bottom figure is for bedrock.

The differences in velocity levels, shown in figures 27 and 28 are at a glance very similar to the velocity level differences for the case with larger diameter cylinders in figure 24. This is a first indication that the reduction of center-center distance could have a similar effect to introducing a larger diameter cylinder (which, coincidentally, reduces the free area between the cylinders to a similar extent). But as discussed in the previous section, this did not seem to give any real reduction of the velocity levels over a broad frequency band, only very narrow band reductions in the higher frequencies for the softer ground types.

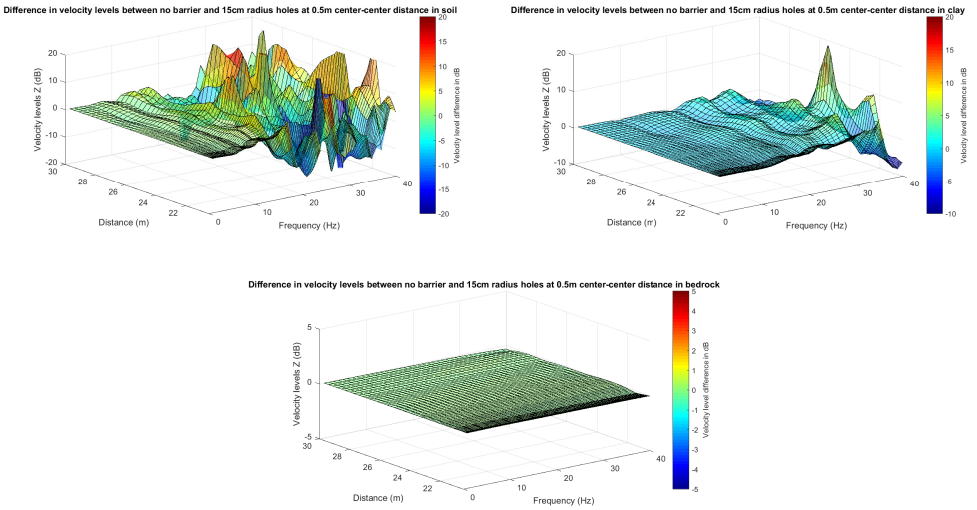

Figure 27: Velocity level difference between all ground types over distance and frequency without any barrier with a **single row of** 15**cm cylinders with a center-center distance of** 0.5**m**.The upper left figure is for soft, sandy soil. The upper right figure is for clay and the bottom figure is for bedrock.

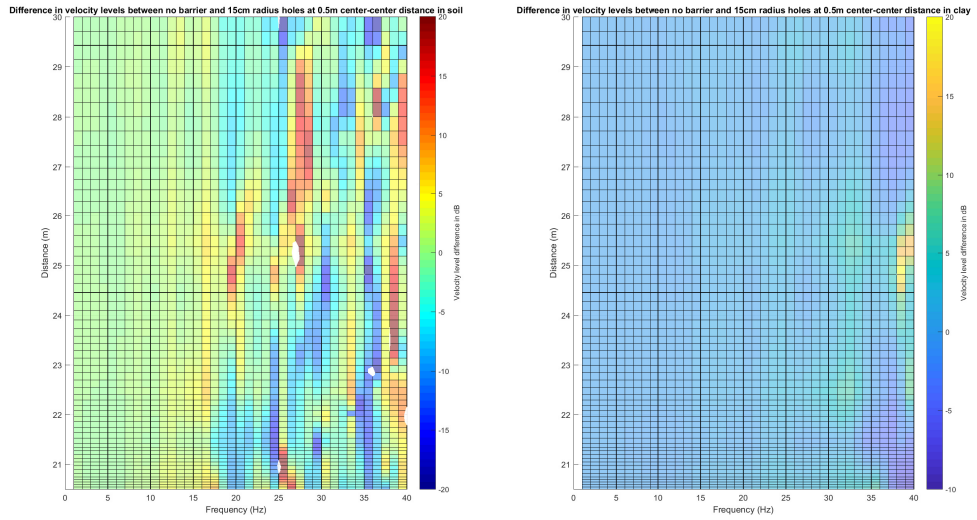

Figure 28: Velocity level difference for softer ground types over distance and frequency with a **single row of** 15**cm cylinders with a center-center distance of** 0.5**m**. The left figure is for soft, sandy soil and the right figure is for clay.

4.1.5 Single row of cylinders, 30cm radius and 0.8m center-center distance.

The combination of a smaller center-center distance and a larger cylinder diameter was studied to see any effect of the propagation of surface waves. The center-center distance was therefore reduced to 0.8m and the radius was doubled to 30cm as compared to the case studied in section 4.1.2. An increased reduction was expected relative to the other cases which had a larger center-center distance or smaller diameter. The velocity levels between 1 to 50Hz over the entire distance can be seen in figure 29. The expected increase in velocity levels at the barrier position can be seen, again indicating some form of absorption. It is not clear from figure 29 if there is any reduction after the barrier position, or any large increase just prior to the barrier position. Like with the previous cases it seems that the only attenuation mechanisms that occur at the barrier position are absorption through energy transfer to the air in the cylinders as well as multiple scattering around the cylinders.

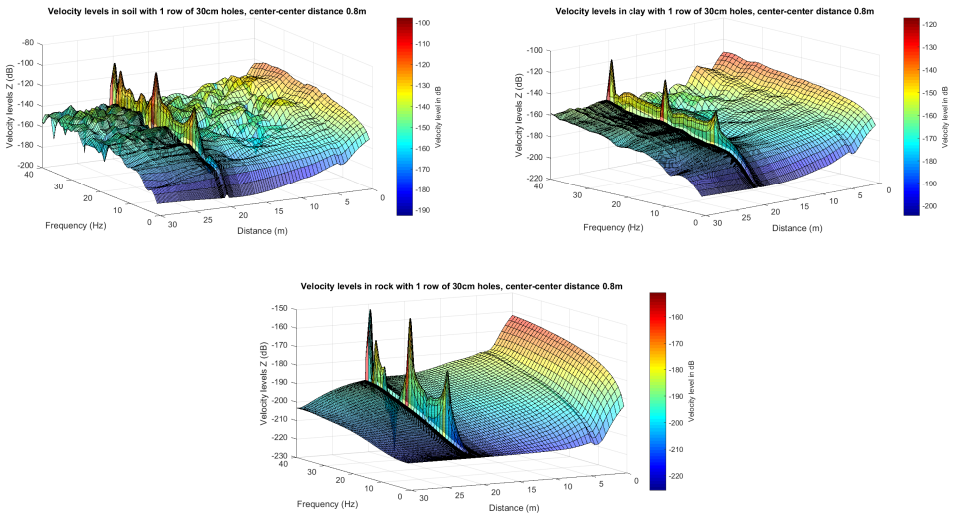

Figure 29: Velocity levels for all ground types over distance and frequency with a **single row of** 30**cm cylinders with a center-center distance of** 0.8**m**. The upper left figure is for soft, sandy soil. The upper right figure is for clay and the bottom figure is for bedrock.

The differences in velocity levels, shown in figures 30 and 31 are similar to the velocity level differences for previously studied cases. This indicates that the effect of larger diameter cylinders or a smaller center-center distance has a minor effect on the reduction of velocity levels over the entire frequency band of interest, but perhaps will have a larger effect on the selective filtering of individual frequencies.

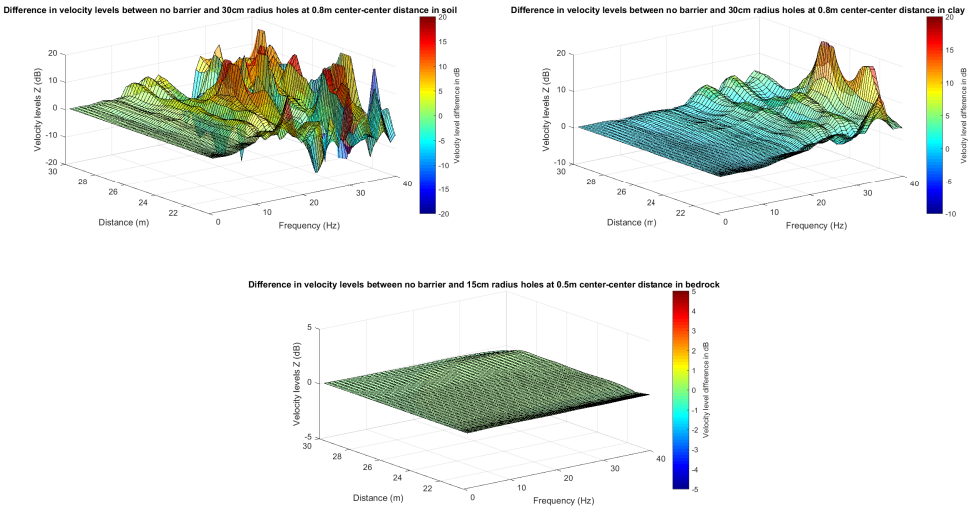

Figure 30: Velocity level difference between all ground types over distance and frequency without any barrier with a **single row of** 30**cm cylinders with a center-center distance of** 0.8**m**. The upper left figure is for soft, sandy soil. The upper right figure is for clay and the bottom figure is for bedrock.

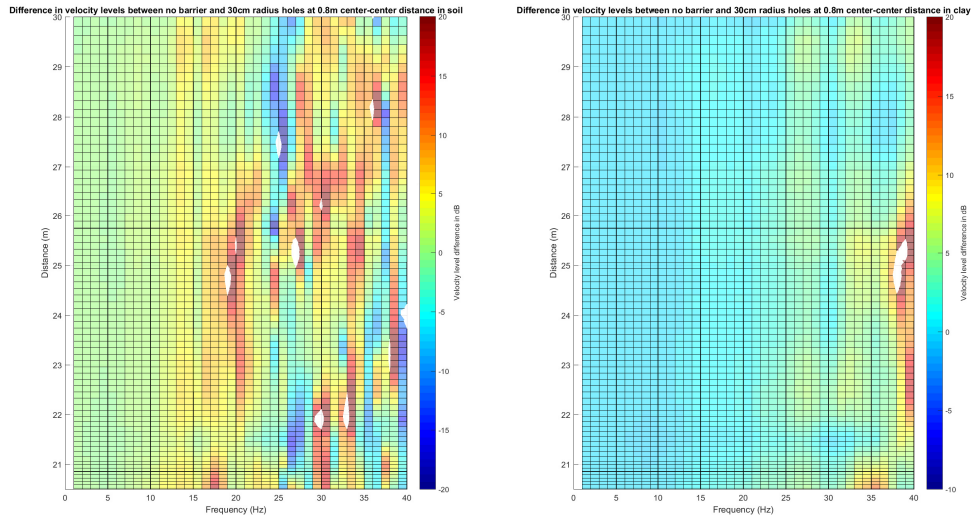

Figure 31: Velocity level difference for softer ground types over distance and frequency with a **single row of** 30**cm cylinders with a center-center distance of** 0.8**m**. The left figure is for soft, sandy soil and the right figure is for clay.

4.1.6 Double row of cylinders, 15cm radius and 1m center-center distance.

As well as a change of cylinder diameter and center-center distance, it was hypothesized that more rows of cylinders could be more effective at attenuating ground vibrations than a single row. This is the same principle as putting more a double layered wall in front of an airborne sound wave in order to increased the reduction index of said wall. A double row of 15cm hollow cylinders was therefore modelled. Following the analogy of the double layered wall, an increase in the reduction was expected when compared to any of the previous cases where only a single layer was present. The velocity levels between 1 to 50Hz over the entire distance can be seen in figure 32. An increase in velocity levels at both barrier positions can be seen, again indicating some form of energy transfer. It is not clear from figure 32 if there is any reduction after the barrier position, or any large increase just prior to the barrier position. Just as with the previous cases it seems that the only attenuation mechanisms that occur at the barrier position are absorption through energy transfer to the air in the cylinders as well as multiple scattering around the cylinders.

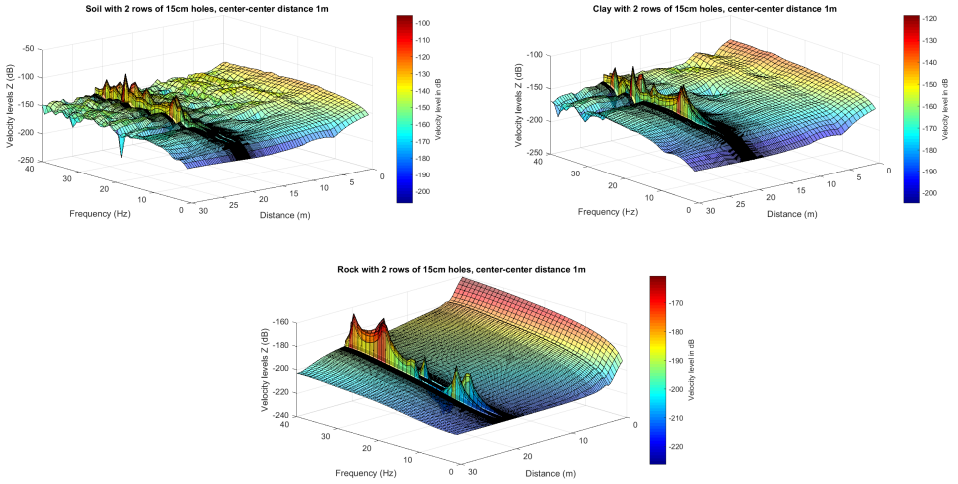

Figure 32: Velocity levels for all ground types over distance and frequency with a **double row of** 15**cm cylinders with a center-center distance of** 1**m**. The upper left figure is for soft, sandy soil. The upper right figure is for clay and the bottom figure is for bedrock.

The differences in velocity levels, shown in figures 33 and 34 are similar to the velocity level differences for previously studied cases, but for the softer ground types there seems to be a real reduction of velocity levels in the higher frequencies.

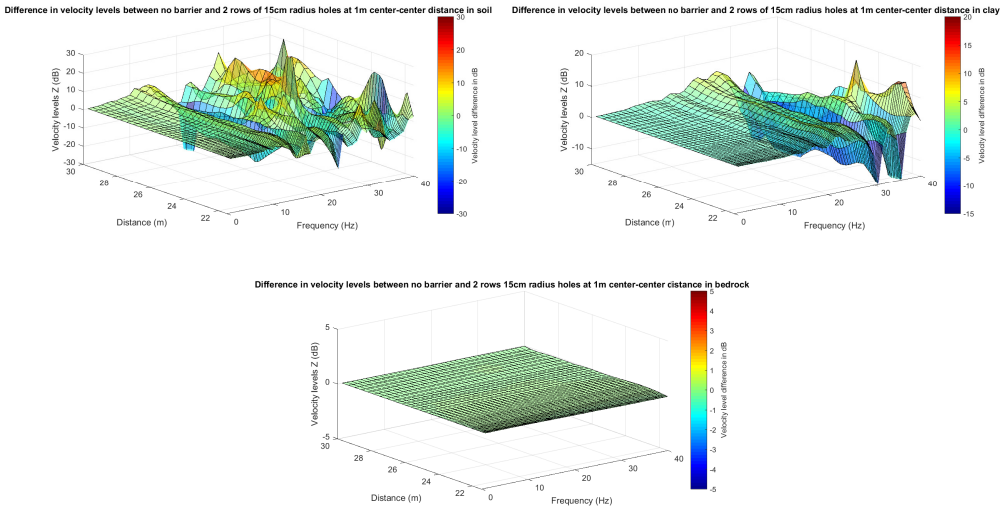

Figure 33: Velocity level difference between all ground types over distance and frequency without any barrier with a **double row of** 15**cm cylinders with a center-center distance of** 1**m**. The upper left figure is for soft, sandy soil. The upper right figure is for clay and the bottom figure is for bedrock.

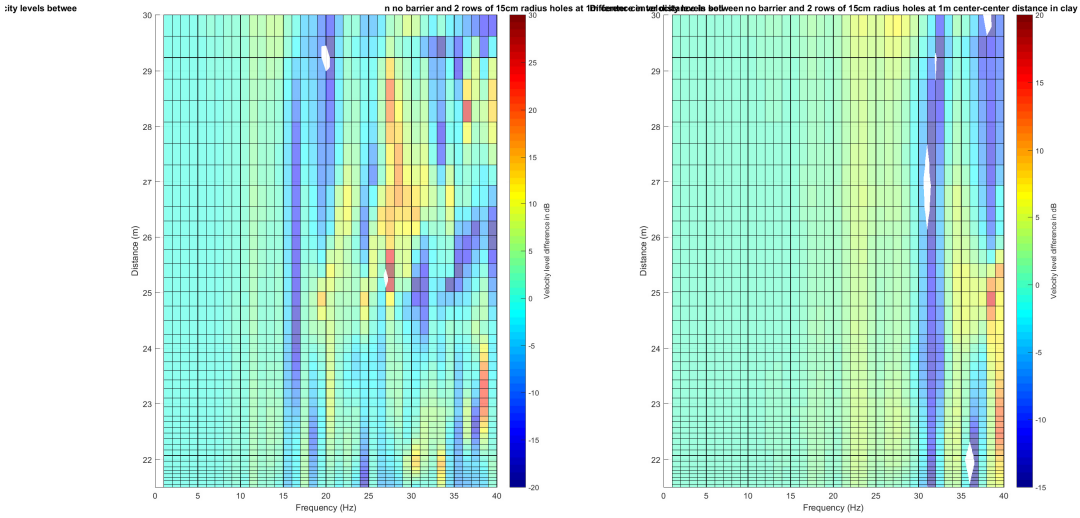

Figure 34: Velocity level difference for softer ground types over distance and frequency with a **double row of** 15**cm cylinders with a center-center distance of** 1**m**. The left figure is for soft, sandy soil and the right figure is for clay.

4.1.7 Four rows of cylinders, 15cm radius and 1m center-center distance.

Since the double row of cylinders seemed to have more of an attenuation effect than a single row, especially in the higher frequencies, four rows of cylinders should double the reduction of velocity levels relative to the double row. Four rows of 15cm was modelled in order to investigate the effect of multiple rows compared with a single or double row. The velocity levels between 1 to 50Hz over the entire distance can be seen in figure 35. An increase in velocity levels at all barrier positions can be seen, again indicating some form of absorption. It should be noted that there is not only an increase but a *decrease* of velocity levels at certain frequencies at certain barrier positions. This could indicate that a node is present at this position, or again some form of interference at certain frequencies. It is not clear from figure 35 if there is any reduction after the barrier position, or any large increase just prior to the barrier position. This is an indication that besides geometrical damping, the only attenuating phenomena to occur at the barrier position are scattering and absorption, whereas for a trench significantly more energy is attenuated through *both reflection and absorption*. It should be noted that scattering can occur in all directions (including back towards the source) and this does reduce the amplitude to an extent, the transfer of energy from the ground to the air in the cylinders would be minimal, which perhaps shows why no significant reduction of the amplitude occurs after the barrier position. The particle velocity could also be increased locally around the cylinder which also could contribute to any reduction, as the loss is proportional to the particle velocity.

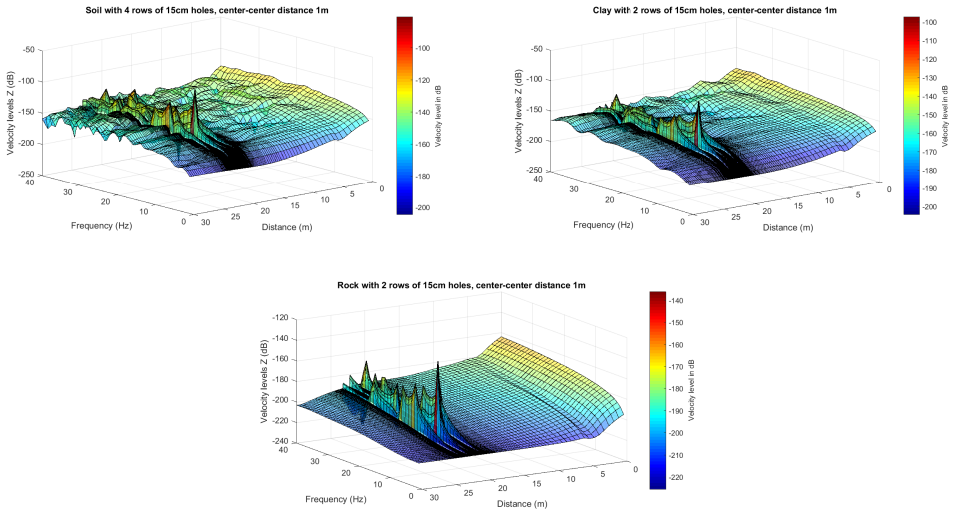

Figure 35: Velocity levels for all ground types over distance and frequency with **four rows of** 15**cm cylinders with a center-center distance of** 1**m**. The upper left figure is for soft, sandy soil. The upper right figure is for clay and the bottom figure is for bedrock.

The difference in velocity levels between the case with four rows and without can be seen in figure 36, with a focus on the softer ground types in figure 37. While some narrow band reduction occurs at the higher frequencies for the softer ground types, indicating some form of filtering, there

is no clear broadband reduction, and the average reduction across all frequency bands is actually negligible, as will be discussed in the next section.

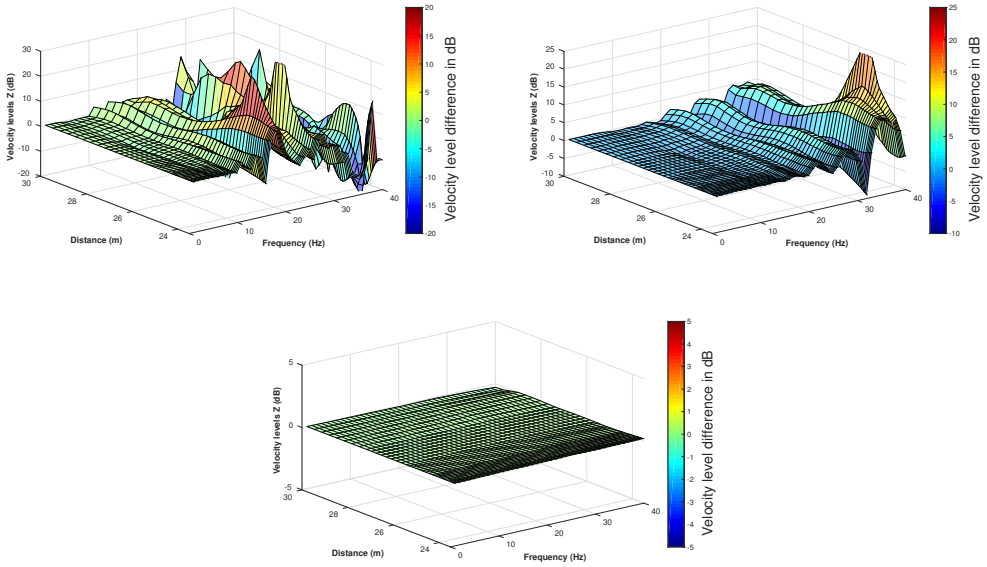

Figure 36: Velocity level difference between all ground types over distance and frequency without any barrier with **four rows of** 15**cm cylinders with a center-center distance of** 1**m**. The upper left figure is for soft, sandy soil. The upper right figure is for clay and the bottom figure is for bedrock.

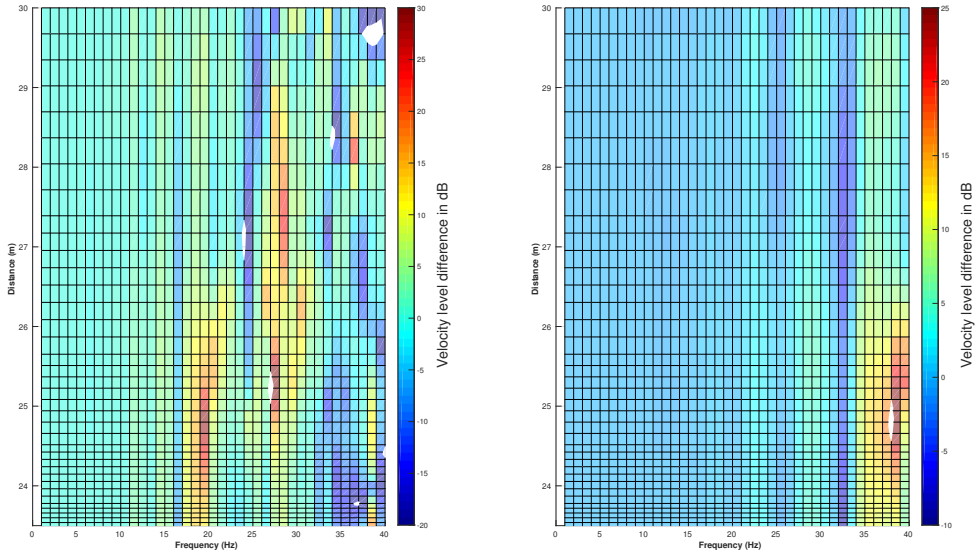

Figure 37: Velocity level difference for softer ground types over distance and frequency with **four rows of** 15**cm cylinders with a center-center distance of** 1**m**. The left figure is for soft, sandy soil and the right figure is for clay.

4.1.8 Cylinders in a circular pattern, holes with 15cm radius, circle radius 3m and segment angle 32.7°.

An array of cylinders in a certain pattern could, in the right conditions, be used to actually form that particular shape. It was therefore hypothesized that a circular array of cylinders *could* give them same effect as a cylinder of the same diameter, in this case 3m. This would obviously depend on the cylinder size and center-center distance. It should be noted that the vector used to model the velocity levels along the distance went straight through the middle of the circular array, but because an odd number of cylinders formed the circular array the vector only went through a single cylinder. The velocity levels between 1 to 50Hz over the entire distance can be seen in figure 38. An increase in velocity levels at the barrier position can be seen, indicating some form of absorption. It is not clear from figure 38 if there is any reduction after the barrier position, or any large increase just prior to the barrier position. This is an indication that besides geometrical damping, the only attenuating phenomena to occur at the barrier position are absorption and multiple scattering around the barrier, whereas for a trench significantly more energy is attenuated through *both reflection and absorption.*

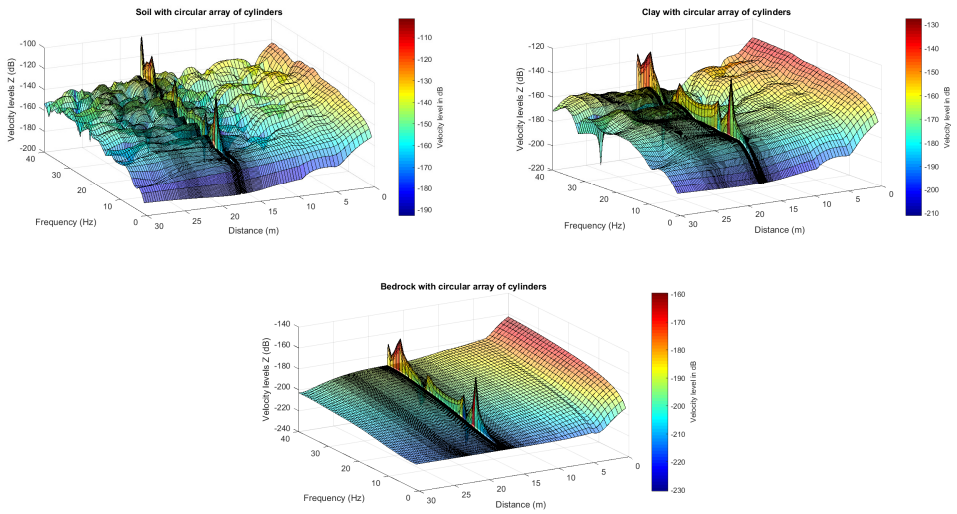

Figure 38: Velocity levels for all ground types over distance and frequency with **cylinders in a circular pattern, holes with** 15**cm radius, circle radius** 3**m and segment angle** 32.7°. The upper left figure is for soft, sandy soil. The upper right figure is for clay and the bottom figure is for bedrock.

The measured reduction for the frequencies of interest for all ground types can be seen in figure 39 and for softer ground types in figure 40. As with all other array types, there seems to be no broadband reduction, only narrow band reduction at certain frequencies and positions after the barrier.

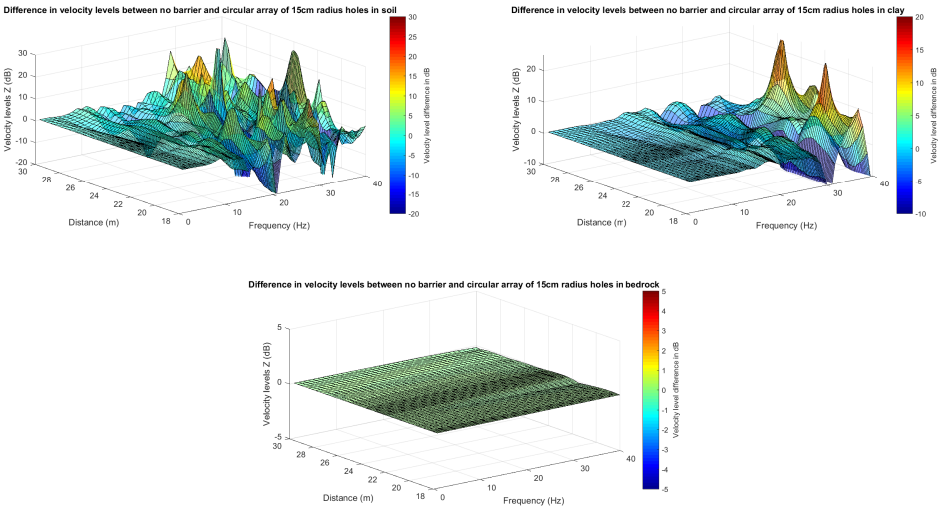

Figure 39: Velocity level difference for all ground types over distance and frequency with **cylinders in a circular pattern, holes with** 15**cm radius, circle radius** 3**m and segment angle** 32.7°. The upper left figure is for soft, sandy soil. The upper right figure is for clay and the bottom figure is for bedrock.

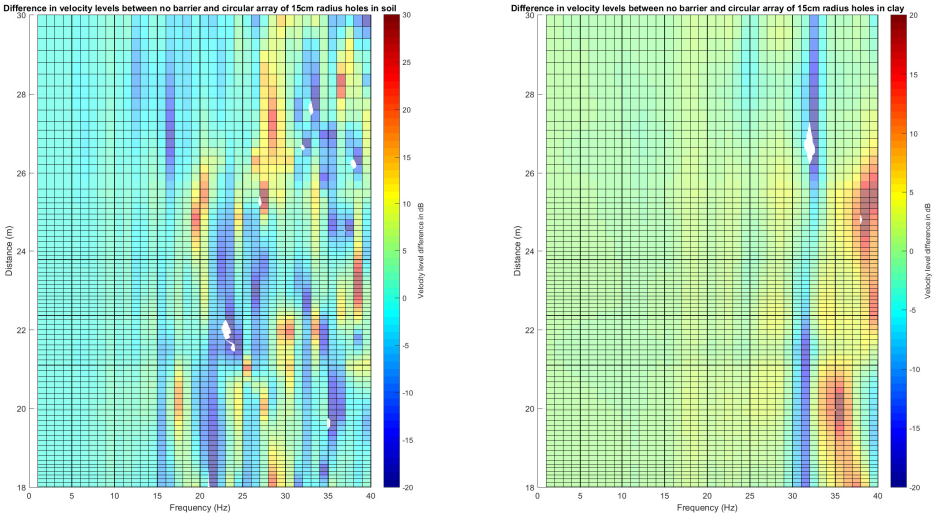

Figure 40: Velocity level difference for softer ground types over distance and frequency with **cylinders in a circular pattern, holes with** 15**cm radius, circle radius** 3**m and segment angle** 32.7°. The left figure is for soft, sandy soil and the right figure is for clay.

It was interesting to observe the propagation of the surface wave in the time domain as it interacted with this particular barrier type. Even though no significant reduction of the displacement field could be observed after the array, there seemed to be an internal reflection *inside* the array, as seen very clearly in figure 41, and in particular in figure 41(c). This phenomena occurred at the higher frequencies, indicating that if the diameter of the array is of a certain integer of a particular frequency, internal reflections can occur inside that particular array. Another barrier of interest would be of a similar type but perhaps half circles of larger diameter cylinders in a tighter pattern.

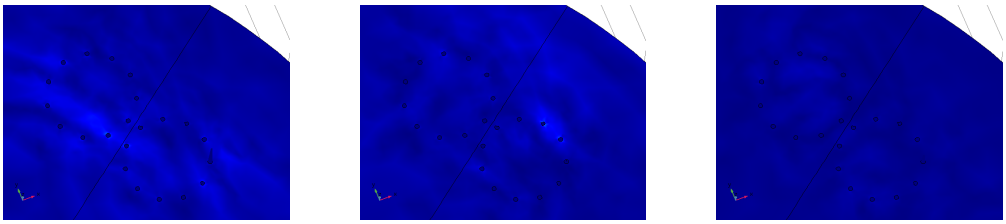

(a) (b) (c)

Figure 41: Time lapse of the wave front hitting the circular array of cylinders.

4.1.9 Compilation of all results

The above sections have discussed the results of the individual barriers without assigning any numerical values to the **total** reduction or **average** reduction in particular frequency bands. So far, only a graphical result has been shown in the form of the difference matrix between each barrier type and the surface velocity levels in the absence of a barrier. This would perhaps be sufficient if a clear reduction could be seen in particular frequency bands, but since the results were very difficult to interpret graphically, numerical values are necessary to complete this analysis of the effectiveness of different barrier types. Table 2 shows the results of this numerical analysis. The average reduction in each 5Hz band has been shown up to 40Hz for a vector at all points after the barrier position, and the total reduction across the entire band has also been presented in the end column. The barrier numbers correspond to those in figure 11.
The trench (barrier 1 in table 2) shows a large reduction across the entire frequency band. This proves that the model works and that the trench is a good choice for a wave barrier, particularly in softer ground types. Interestingly, this was the only barrier type that showed a significant reduction of the velocity levels below 20Hz. It should be noted, however, that no barriers provided any significant reduction for **bedrock**. This is most likely because the velocity levels were too low to start with (about 40dB below the velocity levels for soft sandy soil), meaning that the attenuation from material damping is far more effective than any wave barrier; as a barrier gives a broadband reduction of between 5 and 6dB, but the more dense, stiffer ground type has a velocity level 40dB below the softest ground type. Another ground type besides **bedrock** should perhaps have been studied.
It would appear that **reflection** has the greatest effect on the reduction of the velocity levels. This is because the difference in results as to when reflection definitely occurred (in the case with the trench) and when reflection did not occur or was not as pronounced as for the situation with the trench (as in all other cases). It should be noted that reflection did not seem to help attenuate

the extremely low frequencies ($f < 5Hz$). For the other barrier types, no broadband reduction was measured for the surface velocity levels for any ground type. This can be seen in any of the reduction figures above, as any negative difference in velocity level in one frequency would have been offset by a positive difference in another frequency (giving the observed dips and peaks). Certain frequency bands for different barrier and ground types do show some significant reduction (barrier type 8 in soil between 21-25Hz, for example), but these desirable results are so uncommon that it seems that arrays of hollow, vertical cylinders are not ideal for reducing the velocity levels of *surface* ground vibrations. In practical cases, where only a small reduction is necessary to fulfill certain regulations, a 1dB reduction does represent a 10% decrease in the velocity level amplitude, meaning that these arrays could be a potential solution for these particular cases.

Table 2: Reduction values across entire frequency band for all barrier types

	Reduction in 0-5Hz band (dB)	**Reduction in 6-10Hz band (dB)**	**Reduction in 11-15Hz band (dB)**	**Reduction in 16-20Hz band (dB)**	**Reduction in 21-25Hz band (dB)**	**Reduction in 26-30Hz band (dB)**	**Reduction in 31-35Hz band (dB)**	**Reduction in 36-40Hz band (dB)**	**Average reduction over entire frequency band (dB)**
Barrier 1 soil	0,27	-4,30	-10,62	-6,99	-8,10	-4,70	-1,79	-0,23	**-4,56**
Barrier 1 clay	-0,16	0,63	-2,64	-6,14	-13,36	-8,36	-7,94	-3,72	**-5,21**
Barrier 1 rock	0,03	0,06	-0,04	-0,21	-0,34	-0,25	-0,27	0,37	**-0,08**
Barrier 2 soil	-0,21	0,23	1,87	3,70	5,80	3,48	-1,31	1,53	**1,89**
Barrier 2 clay	-0,02	-0,13	0,18	0,60	1,42	2,84	2,26	2,79	**1,24**
Barrier 2 rock	0,00	-0,01	-0,02	-0,03	-0,03	-0,04	-0,05	-0,05	**-0,03**
Barrier 3 soil	-0,22	-0,17	-0,21	0,84	1,11	-0,22	-0,14	3,18	**0,52**
Barrier 3 clay	-0,04	-0,29	-0,47	0,00	0,39	-0,47	0,75	2,97	**0,35**
Barrier 3 rock	0,00	-0,01	-0,03	-0,05	-0,07	-0,07	-0,09	-0,16	**-0,06**
Barrier 4 soil	-0,09	0,37	1,58	-0,71	-2,24	-1,14	-3,51	2,18	**-0,44**
Barrier 4 clay	0,01	-0,14	0,10	0,56	1,31	1,22	1,83	-0,44	**0,56**
Barrier 4 rock	0,00	0,01	0,01	0,00	0,00	-0,01	-0,03	-0,07	**-0,01**
Barrier 5 soil	0,01	0,91	3,24	6,19	0,24	4,00	4,59	-0,40	**2,35**
Barrier 5 clay	0,06	-0,01	0,55	1,12	2,27	3,17	4,43	7,25	**2,36**
Barrier 5 rock	0,00	0,02	0,02	0,02	0,05	0,06	0,05	0,02	**0,03**
Barrier 6 soil	0,06	0,61	1,46	-2,58	0,11	3,08	-0,85	-0,37	**0,19**
Barrier 6 clay	0,05	0,06	0,26	1,13	2,86	0,56	-2,49	-0,03	**0,30**
Barrier 6 rock	0,00	0,01	0,01	0,00	0,01	0,01	-0,01	-0,01	**0,00**
Barrier 7 soil	0,05	-0,05	2,29	5,72	0,11	6,41	-3,52	-4,67	**0,79**
Barrier 7 clay	0,07	0,05	-0,10	0,32	1,17	2,78	2,37	8,15	**1,85**
Barrier 7 rock	0,00	0,01	0,03	0,04	0,06	0,07	0,05	0,03	**0,04**
Barrier 8 soil	-0,09	0,43	-0,40	1,24	-3,58	3,39	-2,04	0,89	**-0,02**
Barrier 8 clay	0,03	-0,08	-0,16	1,02	0,41	-0,03	-0,52	3,30	**0,50**
Barrier 8 rock	0,00	0,02	0,02	0,02	0,02	0,02	0,01	-0,01	**0,01**

4.1.10 The effects on body waves

The barrier types studied showed minimal or no reduction in the velocity levels of the *surface* waves, it was deemed appropriate to see the effects of the barrier types on body waves. A deep concrete foundation was simulated in soil 5m after the barrier. The concrete foundation was a 1 by 1m square which was 6m deep. This was so the body waves would interact with the foundation below the surface, in order to observe any effect the barrier would have on any body waves below the surface. This model can be seen in figure 42.

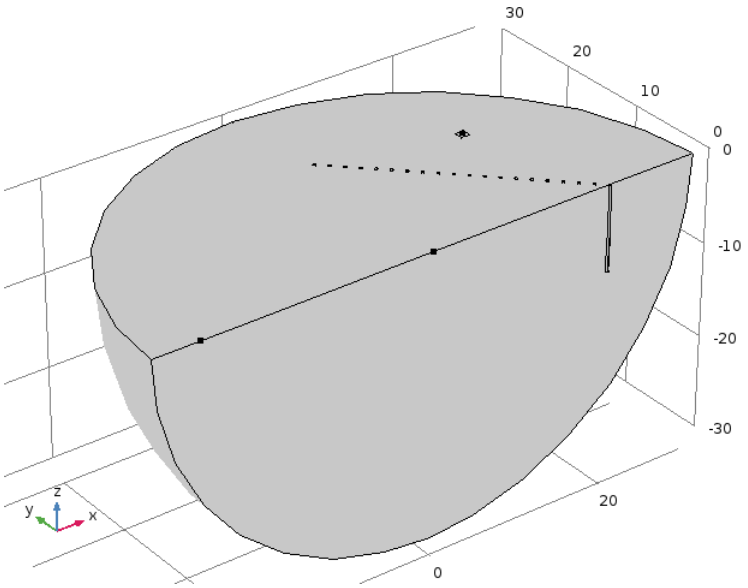

Figure 42: The model to test for the effect of an array of hollow cylinders on body waves. The concrete foundation can be seen after the barrier position

The barrier of choice for this simulation was the 15cm radius cylinders at a 1m distance. This was just to determine if there was any effect to be had by implementing an array of cylinders. The velocity levels in the Z-direction at a point in the center of the surface of the foundation was then found for the frequency band 1 through 40Hz for the cases with and without a barrier, in order to observe any reduction. The result of this simulation can be seen in figure 43.

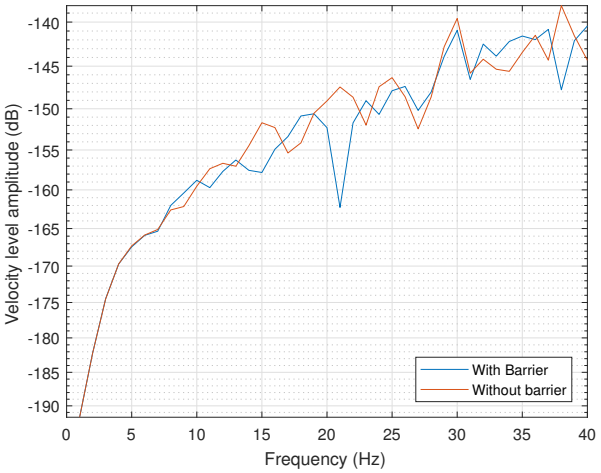

Figure 43: The measured velocity level amplitude on the surface of the concrete foundation with and without the wave barrier.

It is clear from figure 43 that the barrier has a clear filtering effect on certain frequencies, as there is no clear broadband reduction, but a large reduction between 20 to 25Hz. This area of study should be researched further in order to optimize the array pattern and cylinder size.

5 Discussion

The results of the executed numerical simulations indicate that vertical arrays of cylinders have no significant effect on the velocity levels of *surface* waves, but there are indications that arrays of vertical cylinders could be used for the reflection, absorption and filtering of body waves. There are a number of reasons why this could be the case.

- The wavelengths for the surface waves are too long to allow for any gaps in the wave barrier if the frequencies that should be attenuated are below 50Hz. This means that the wavelengths need to be taken into careful consideration when choosing the center-center distance, but this limits the effective frequency range to the higher frequencies. As it is the lower frequencies that are the most damaging and disturbing to buildings it seems that a trench or full wave barrier is the best and most economical solution for attenuating low frequency surface waves.

- The shape of the units forming the arrays could be allowing for the attenuation of the surface waves *around* the individual units with minimal energy loss. It was interesting to see the difference in velocity levels immediately before the barrier positions for all the arrays of cylinders. Unlike for the trench, which showed a significant increase in velocity level at the positions before the trench position, this could not be observed for any of the array types, indicating a complete lack of reflection. It could be that the shape of the cylinders gives an impedance mismatch and therefore acts as a wave-guide. It would be interesting to see other shapes besides cylinders.

- Deep, vertical wave barriers are not optimal for the attenuation of vertically polarized surface waves. As discussed in section 2, Rayleigh waves are confined to the surface and decay rapidly with depth. Therefore, a shallow trench would be the optimal wave barrier for this wave type. An array of vertical cylinders *could* be more effective for horizontally polarized surface waves, otherwise known as *Love waves*.

Despite the reduction levels from the arrays being significantly lower than the trench, for some array types there is some narrow-band reduction (up to -3dB) and in some cases a broadband reduction of up to -2dB. While small, this still represents a 10-30% reduction in the velocity level amplitude, which means that this method could potentially be used if only a small reduction is necessary to fulfill the relevant regulations.
COMSOL multiphysics was an extremely good tool to use for studying the propagation of ground vibrations in an elastic half space. It was particularly interesting to observe the propogation of the different wave types in the time domain, which gave valuable input into this project. The flexibility of COMSOL allowed for small, but important changes to the model without having to do too much work. The actual geometrical model was perhaps too small for the desired purpose, and a doubling of the radius would not have added too much to the computation time if the mesh size was kept large enough. This size mismatch was especially true for the harder ground types which had longer wavelengths. For this project, the module *Solid mechanics* was used. But there are perhaps better modules such as the *acoustics* module, which has better features such as a non-reflective layer, instead of a low-reflective boundary, which had certain limitations as discussed in section 4.
The choice of ground types was intended to show the entire span of densities and stiffness's that can be found in nature. But the choice of bedrock was perhaps misguided, as it was far stiffer and denser than the other ground types chosen. Which was seen by the significant difference in velocity levels without any barrier (figure 12) and the apparent lack of effect of any barrier type. While this

showed that many of the results did not show any significant effect for bedrock, it shows just how effective stiffening of the ground can be for attenuating ground vibrations.
Despite the results showing that there was no significant reduction achieved for surface waves, it seems that arrays of cylinders could be effective at filtering body waves. As body waves interact with deep foundations (which are more often used in areas with soft soil), this could prove to be extremely useful. If the excitation is underground, such as from a subway, an array of cylinders could be constructed to attenuate these body waves before they reach the underside and/or foundations of surrounding buildings.
If a similar project was to be performed again, the focus should be on the effects of these hollow cylinders on body waves, including changing the angle of incidence, size and center-center distance. The position of the excitation would also have been interesting to study, perhaps comparing an underground to surface excitation. With more time a layered system would also have been interesting to analyze, with the aim of seeing if any barrier type is more effective for attenuating Love waves.
After learning about what kind of barriers are more effective at attenuating different wave types, it seems that a hybrid of a trench and array of cylinders could be used as a more economical and effective approach to attenuating all wave types in areas where ground vibrations are problematic. A concept for this wave barrier can be seen in figure 44. The top of the wave barrier is a shallow trench or wall, which is primarily for reflecting incoming Rayleigh and Love waves. The coupled array of hollow or filled cylinders is used for filtering incoming body waves. This would be far more economically feasible than a deep wall or trench. The array of cylinders could be angled in order to reflect more of the energy of the incident body waves.

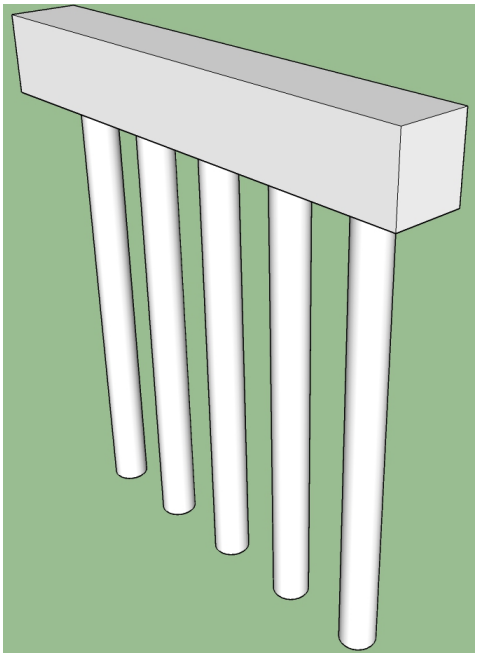

Figure 44: Concept wave barrier

6 Conclusion

The purpose of this project; to determine if it is possible to filter ground vibrations using an array of hollow cylinders in the wave fronts path, was achieved to an extent. Filtering of individual frequencies was indeed observed but no function between the filtered frequencies and the cylinder size or disposition could be calculated. It also was discovered that these arrays seems to be far more effective at attenuating body waves instead of surface waves.
The aims of this study were as follows:

- To produce a theoretical and mathematical framework to test if the theory works. This can be through analytical calculations or numerical simulations.
- To test the theory in real world conditions and compare the measured results to the theoretical and mathematical framework.
- To optimize any solution to maximize the cost to benefit ratio.
- Analyse any potential use for the method in question.

Unfortunately, the aim to test the theory in real world conditions could not be accomplished because of economic and logistical difficulties which could not be overcome. But the first, third and fourth aims have been accomplished. A theoretical and numerical framework to test the theory was done through simulating these barrier types in COMSOL, and as no solution involving arrays of cylinders did not give any real reduction, no optimization could be performed. The use of these arrays has been analyzed based on the final simulation of the deep foundation which gave more promising results, and a concept for a wave barrier has been sketched.
Future study in the filtering of ground vibrations should focus on *body* waves instead of surface waves. It is important since in areas of soft ground, where deep foundations are needed, these body waves couple to these deep foundations and propagate up through the load bearing structure and can, in this manner, propagate further up or into a building than any wave caused by the incoming Rayleigh wave. It would also be interesting to see what happens in layered systems where differently polarized shear waves occur, as well as the effects of angle of incidence on a barrier. In addition, different materials should also be simulated in order to study the effects of different impedance changed on the different attenuation mechanisms for different ground types.

References

[1] Göran Sällfors. *Geoteknik*. Chalmers Tekniska Högskolan, 2009. ISBN: 6484564865.

[2] F.E. Richart Jr & J.R. Hall Jr & R.D. Woods. *Vibrations of soils and foundations*. Prentice Hall INC, 1970. ISBN: 13-941716-8.

[3] *Geomechanics: Bridging the Gap from Geophysics to Engineering in Unconventional Reservoirs*. URL: `http://csegrecorder.com/articles/view/geomechanics-bridging-the-gap-from-geophysics-to-engineering` (visited on 02/09/2017).

[4] *Siesmic Refraction Surveying*. URL: `http://www.ukm.my/rahim/Seismic%20Refraction%20Surveying.htm` (visited on 02/17/2017).

[5] *Attenuation of ground vibrations from pile driving*. URL: `https://www.geplus.co.uk/download?ac=1429226`.

[6] *Sensing, Analyzing, and Acting in the First Moments of an Earthquake*. URL: `http://www.analog.com/en/analog-dialogue/articles/sensing-analyzing-and-acting-during-an-earthquake.html` (visited on 02/17/2017).

[7] *Gravity Gradient Noise from Ground Waves*. URL: `http://www.johnstonsarchive.net/relativity/ggpresentation.html` (visited on 05/30/2017).

[8] *Monitoring the temporal changes of reservoirs by means of wide-angle reflection and refraction of S-wave in an offshore region*. URL: `https://www.researchgate.net/figure/281440175_fig4_Figure-4-Schematics-of-reflection-and-refraction-of-P-wave-and-two-type-S-waves-ie` (visited on 02/21/2017).

[9] Bengtsson & Moritz Möller Larsson. *Geodynamik i praktiken*. Statens geotekniska institut (SGI) 581 93 Linköping, 2000.

[10] Rainer M Massarsch. *Ground Vibration Isolation Using Gas Cushions*. Geoengineering SA, Waterloo, Belgium, 1991.

[11] *Interview with Alf Ekblad*. 2017.

[12] Ashwani & Soni. *Foundation Vibration Isolation Methods*. Dept. of Civil Engineering National Institute Technology Kurukshetra-136119 INDIA, 2007.

[13] COMSOL Multiphysics. *COMSOL Multiphysics 5.2 online manual*. 2016.

Appendix

```
%% material info
f=1:50
%v=linspace(0, 0.5);
                                                        % poissons
    ratio
v_lera=0.49;
v_clay=0.48;
v_rock=0.4;
rho_lera=1600;
rho_clay=2125;
rho_rock=2600;
E_lera=63.7e6;
E_clay=340e6;
E_rock=8809e6;
omega=2*pi.*f;
G_lera=E_lera/(2+2*v_lera)
G_clay=E_clay/(2+2*v_clay)
G_rock=E_rock/(2+2*v_rock)
%G=E./(2+2.*v);
                                                              %lames
     constant shear
%lambda=(v.*E)./((1+v).*(1-2.*v));
                                                    %lames constant
lambda_lera=(v_lera*E_lera)/((1+v_lera)*(1-2*v_lera))
lambda_clay=(v_clay*E_clay)/((1+v_clay)*(1-2*v_clay))
lambda_rock=(v_rock*E_rock)/((1+v_rock)*(1-2*v_rock))

%% wave speeds
%V_p= sqrt((lambda + 2*G)./rho);
                                                  %wave speed
    compression
%V_s= sqrt(G./rho);
                                                              %wave
    speed shear

Cplera=sqrt((E_lera*(1+v_lera))/(rho_lera*(1-2*v_lera)*(1+v_lera)))
Cslera=sqrt(E_lera/(rho_lera*2*(1+v_lera)))
Cpclay=sqrt((E_clay*(1+v_clay))/(rho_clay*(1-2*v_clay)*(1+v_clay)))
Csclay=sqrt(E_clay/(rho_clay*2*(1+v_clay)))
Cprock=sqrt((E_rock*(1+v_rock))/(rho_rock*(1-2*v_rock)*(1+v_rock)))
Csrock=sqrt(E_rock/(rho_rock*2*(1+v_rock)))

%% wave lengths
WL_p_l=Cplera./f;
```

```
WL_s_l=Cslera./f;
WL_p_c=Cpclay./f;
WL_s_c=Csclay./f;
WL_p_r=Cprock./f;
WL_s_r=Csrock./f;

%L_r = (2*pi*V_r)/omega
figure(1)
semilogy(f,WL_p_l,'r')
hold on
semilogy(f,WL_p_c,'g')
hold on
semilogy(f,WL_p_r,'b')
hold on
semilogy(f,WL_s_l,'--r')
hold on
semilogy(f,WL_s_c,'--g')
hold on
semilogy(f,WL_s_r,'--b')
legend("P-wavelength soft sandy soil","P-wavelength clay", "P-
    wavelength bedrock","S-wavelength soft sandy soil","S-wavelength
    clay", "S-wavelength bedrock")
xlabel("Frequency (Hz)")
ylabel("Wavelength (m)")
title('Wavelength over frequency for P-and S waves in soil, clay and
    bedrock')

%%

V_poisson=[0:0.01:0.5]
Cp=sqrt((E_lera.*(1+V_poisson))./(rho_lera*(1-2.*V_poisson).*(1+
    V_poisson)))
Cs=sqrt(E_lera./(rho_lera*2.*(1+V_poisson)))
Xpoisson=[0, 0.5]
Ypoisson=[0.8 , 1]


plot(V_poisson, Cp./Cs, V_poisson, Cs./Cs, Xpoisson, Ypoisson)
xlim([0,0.5])
ylim([0,6])
xlabel('Poissons ratio, v')
ylabel('Values of V/Vs')
title('Relation between Poissons ratio and body/surface wave velocities
    ')
legend('P- wave', 'S- wave', 'R-wave','Location','northwest')

```

```
77 f=[1:1:40];
78 %with barrier
79 V_soil_close_w_barrier=reshape(close_w_barrier,[40,4]);
80 V_soil_close_w_barrier_tot=(V_soil_close_wo_barrier(:,1)+
       V_soil_close_wo_barrier(:,2)+V_soil_close_wo_barrier(:,3)+
       V_soil_close_wo_barrier(:,4))/4
81
82 V_soil_far_w_barrier=reshape(far_w_barrier,[40,4]);
83 V_soil_far_w_barrier_tot=(20*log10(abs(V_soil_far_w_barrier(:,1)+
       V_soil_far_w_barrier(:,2)+V_soil_far_w_barrier(:,3)+
       V_soil_far_w_barrier(:,4))/4))
84
85 %without barrier
86 V_soil_close_wo_barrier=reshape(close_wo_barrier,[40,4]);
87 V_soil_close_w0_barrier_tot=(V_soil_close_wo_barrier(:,1)+
       V_soil_close_wo_barrier(:,2)+V_soil_close_wo_barrier(:,3)+
       V_soil_close_wo_barrier(:,4))/4
88
89 V_soil_far_wo_barrier=reshape(far_wo_barrier,[40,4]);
90 V_soil_far_wo_barrier_tot=(20*log10(abs(V_soil_far_wo_barrier(:,1)+
       V_soil_far_wo_barrier(:,2)+V_soil_far_wo_barrier(:,3)+
       V_soil_far_wo_barrier(:,4))/4))
91
92
93 semilogy(freq, V_soil_far_w_barrier_tot, freq,
       V_soil_far_wo_barrier_tot)
94 grid on
95 xlabel('Frequency (Hz)')
96 ylabel('Velocity level amplitude (dB)')
97 legend('With Barrier','Without barrier','Location','southeast')
98
99 reduction=(V_soil_far_w_barrier_tot-V_soil_far_wo_barrier_tot)'
100 avg_tot_red=mean(V_soil_far_w_barrier_tot-V_soil_far_wo_barrier_tot)
101
102
103 %%
104
105 %soil
106 V_soil_wo_barrier=reshape(vel_soil_wo_barrier,[64,40]);
107 V_X_soil_wo_barrier=reshape(vel_X_soil_wo_barrier,[64,40]);
108 V_soil_trench=reshape(vel_soil_trench,[154,40]);
109 V_X_soil_trench=reshape(vel_X_soil_trench,[154,40]);
110 V_soil_holes=reshape(vel_soil_holes,[154,40]);
111 V_soil_large_holes=reshape(vel_soil_large_holes,[136,40]);
112 V_X_soil_large_holes=reshape(vel_x_soil_large_holes,[136,40]);
113 V_x_soil_holes=reshape(vel_x_soil_holes,[154,40]);
```

```
V_soil_dbl_row=reshape(vel_dbl_row_holes_soil1,[154,40]);
V_soil_4_row=reshape(vel_4_row_soil,[201,40]);
V_soil_tight_holes=reshape(vel_small_holes_tight_soil,[163,40]);
V_soil_tight_large_holes=reshape(vel_large_holes_tight_soil,[145,40]);
V_soil_circular_barrier=reshape(vel_circ_soil,[163,40]);

%clay
V_clay_wo_barrier=reshape(vel_clay_wo_barrier,[64, 40]);
V_X_clay_wo_barrier=reshape(vel_X_clay_wo_barrier,[64,40]);
V_clay_trench=reshape(vel_clay_trench,[154, 40]);
V_X_clay_trench=reshape(vel_X_clay_trench,[154, 40]);
V_clay_holes=reshape(vel_clay_holes,[154,40]);
V_clay_large_holes=reshape(vel_clay_large_holes,[136,40]);
V_X_clay_large_holes=reshape(vel_x_clay_large_holes,[136,40]);
V_x_clay_holes=reshape(vel_x_clay_holes,[154,40]);
V_clay_dbl_row=reshape(vel_dbl_row_holes_clay1,[154,40]);
V_clay_4_row=reshape(vel_4_row_holes_clay,[201,40]);
V_clay_tight_holes=reshape(vel_small_holes_tight_clay,[163,40]);
V_clay_tight_large_holes=reshape(vel_large_holes_tight_clay,[145,40]);
V_clay_circular_barrier=reshape(vel_circ_clay,[163,40]);

%rock
V_rock_wo_barrier=reshape(vel_rock_wo_barrier,[64,40]);
V_X_bedrock_wo_barrier=reshape(vel_X_bedrock_wo_barrier,[64, 40]);
V_rock_trench=reshape(vel_rock_trench,[154,40]);
V_rock_holes=reshape(vel_rock_holes,[154,40]);
V_rock_large_holes=reshape(vel_rock_large_holes,[136,40]);
V_X_rock_large_holes=reshape(vel_x_rock_large_holes,[136,40]);
V_x_rock_holes=reshape(vel_x_rock_holes,[154,40]);
V_x_rock_trench=reshape(vel_x_rock_trench,[154,40]);
V_rock_dbl_row=reshape(vel_dbl_row_holes_rock,[193,40]);
V_rock_4_row=reshape(vel_4_row_holes_rock,[201,40]);
V_rock_tight_holes=reshape(vel_rock_holes_tight,[163,40]);
V_rock_tight_large_holes=reshape(vel_large_holes_tight_rock,[145,40]);
V_rock_circular_barrier=reshape(vel_circ_rock,[163,40]);

%% trying to use interp2 function
%original soil surf
figure(30)
[Xorg,Yorg]=meshgrid(1:40,1:64);
surf(Xorg,Yorg,Z)
%%

figure(18)          %soil velocity level for trench or holes/no barrier
[X1,Y1]=meshgrid(1:40, distance_wo_barrier);
[Xq,Yq]=meshgrid(1:40, distance_trench);
```

```
[Xj,Yj]=meshgrid(1:40, distance_large_holes);
[Xv,Yv]=meshgrid(1:40, distance_small_holes_tight);
[Xlht,Ylht]=meshgrid(1:40, distance_large_holes_tight);
[X4r,Y4r]=meshgrid(1:40, distance_4_row);
[X2r,Y2r]=meshgrid(1:40, distance_dbl_row);
[X2r1,Y2r1]=meshgrid(1:40, distance_dbl_row1);
[Xcirc, Ycirc]=meshgrid(1:40, distance_circ);
%[Xcr, Ycr]=meshgrid(1:40, distance_circ_rock);
Z=20*log10(abs(V_soil_wo_barrier));
Vq=interp2(X1,Y1,Z,Xq,Yq);
surf(Xq,Yq,Vq)
% matrix Vq is now correct

%soil velocity level for large holes/no barrier
[Xq1,Yq1]=meshgrid(1:40,distance_large_holes);
Vq1=interp2(X1,Y1,Z,Xj,Yj);

%soil velocity level for small tight holes
Vsht=interp2(X1,Y1,Z,Xv,Yv);

%soil velocity level for large tight holes
Vlht=interp2(X1,Y1,Z,Xlht,Ylht);

%soil velocity level for double row
Vs2r=interp2(X1,Y1,Z,X2r,Y2r);
Vs2r1=interp2(X1,Y1,Z,X2r1,Y2r1);

%soil velocity level for 4 row
Vs4r=interp2(X1,Y1,Z,X4r,Y4r);

%soil velocity level for circle
Vscirc=interp2(X1,Y1,Z,Xcirc,Ycirc);

%clay velocity level for trench or holes/no barrier
Zc=20*log10(abs(V_clay_wo_barrier));
Vc1=interp2(X1,Y1,Zc,Xq,Yq);

%clay velocity level for large holes/no barrier
Vc2=interp2(X1,Y1,Zc,Xj,Yj);

%clay velocity level for small tight holes
Vc3=interp2(X1,Y1,Zc,Xv,Yv);

%clay velocity level for large tight holes
Vc4=interp2(X1,Y1,Zc,Xlht,Ylht);

```

```
206 %clay velocity level for dbl row
207 Vc5=interp2(X1,Y1,Zc,X2r1,Y2r1);
208
209 %clay velocity level for 4 row
210 Vc6=interp2(X1,Y1,Zc,X4r,Y4r);
211
212 %clay velocity level for circ
213 Vc7=interp2(X1,Y1,Zc,Xcirc,Ycirc);
214
215 %rock velocity level for trench or holes/no barrier
216 Zr=20*log10(abs(V_rock_wo_barrier));
217 Vr1=interp2(X1,Y1,Zr,Xq,Yq);
218
219 %rock velocity level for large holes
220 Vr2=interp2(X1,Y1,Zr,Xj,Yj)
221
222 %rock velocity level for small tight holes
223 Vr3=interp2(X1,Y1,Zr,Xv,Yv);
224
225 %rock velocity level for large tight holes
226 Vr4=interp2(X1,Y1,Zr,Xlht,Ylht);
227
228 %rock velocity level for 2 rows
229 Vr5=interp2(X1,Y1,Zr,X2r,Y2r);
230
231 %clay velocity level for 4 rows
232 Vr6=interp2(X1,Y1,Zr,X4r,Y4r);
233
234 %rock velocity level for circ
235 Vr7=interp2(X1,Y1,Zr,Xcirc,Ycirc);
236
237
238 %%
239 surf(Xq,Yq,Vr1)
240 hold on
241 surf(X,Y,Zrock,'FaceAlpha',0.5)
242
243 %rock velocity level for large holes/no barrier
244 Vr2=interp2(X1,Y1,Zr,Xq1,Yq1);
245
246
247
248
249
250
251 %%
```

```
252 f1=1:40
253
254 avg=[f1; Avg_trench_soil; Avg_trench_clay; Avg_trench_rock;
        Avg_holes_soil; Avg_holes_clay; Avg_holes_rock;
255      Avg_Lholes_soil; Avg_Lholes_clay; Avg_Lholes_rock;
             Avg_sthholes_soil; Avg_sthholes_clay; Avg_sthholes_rock;
256      Avg_lthholes_soil; Avg_lthholes_clay; Avg_lthholes_rock;
             Avg_2rholes_soil; Avg_2rholes_clay; Avg_2rholes_rock;
257      Avg_4rholes_soil; Avg_4rholes_clay; Avg_4rholes_rock;
             Avg_circholes_soil; Avg_circholes_clay; Avg_circholes_rock]
258
259
260
261
262
263
264
265
266
267
268
269
270
271
272
273
274
275
276
277
278
279
280
281
282
283
284
285
286
287
288
289
290
291 %% notes
292
293
```

```
294 %15 Hz looks wierd
295 %for 15cm holes at 1m cc, start getting a reduction above 18 Hz
296 %(18,22,23,24,25, 26, 28,29, 30)
297 % seems there could be some distructive or constructive interference
        from
298 % the refraction around the holes along the direction of the wave front
299
300 %% 3D FIGURES BELOW
301 %difference between circ and no barrier
302 %distance vectors need to be the same! (30m)
303
304 subplot(1,2,1)
305 [X4,Y4]=meshgrid(1:40,distance_circ);
306 Z_comp_soil_circ=(20*log10(abs(V_soil_circular_barrier)))-Vscirc;
307 surf(X4,Y4,Z_comp_soil_circ,'FaceAlpha',0.5)
308 ylim([18 30])
309 zlim([-20 30])
310 caxis([-30,20])
311 title('Difference in velocity levels between no barrier and circular
        array of 15cm radius holes in soil')
312 c = colorbar;
313 c.Label.String = 'Velocity level difference in dB';
314 xlabel('Frequency (Hz)')
315 ylabel('Distance (m)')
316 zlabel('Velocity levels Z (dB)')
317 subplot(1,2,2)
318 %[X4,Y4]=meshgrid(1:40,distance_small_holes_tight);
319 Z_comp_clay_circ=(20*log10(abs(V_clay_circular_barrier)))-Vc7;
320 surf(X4,Y4,Z_comp_clay_circ,'FaceAlpha',0.5)
321 ylim([18 30])
322 zlim([-20 25])
323 caxis([-30,20])
324 title('Difference in velocity levels between no barrier and circular
        array of 15cm radius holes in clay')
325 c = colorbar;
326 c.Label.String = 'Velocity level difference in dB';
327 xlabel('Frequency (Hz)')
328 ylabel('Distance (m)')
329 zlabel('Velocity levels Z (dB)')
330 subplot(2,2,3.5)       %difference between large holes and no barrier -
        something is wrong
331 %[X4,Y4]=meshgrid(1:40,linspace(0,30,136));
332 %[X4,Y4]=meshgrid(1:40,distance_circ)
333 Z_comp_rock_circ=(20*log10(abs(V_rock_circular_barrier)))-Vr7;
334 surf(X4,Y4,Z_comp_rock_circ,'FaceAlpha',0.5)
335 ylim([18 30])
```

```
zlim([-5 5])
caxis([-20,10])
title('Difference in velocity levels between no barrier and circular array of 15cm radius holes in bedrock')
c = colorbar;
c.Label.String = 'Velocity level difference in dB';
xlabel('Frequency (Hz)')
ylabel('Distance (m)')
zlabel('Velocity levels Z (dB)')

% average reduction values
circholes_soil_matrix=Z_comp_soil_circ(82:163,1:40);
circholes_clay_matrix=Z_comp_clay_circ(82:163,1:40);
circholes_rock_matrix=Z_comp_rock_circ(82:163,1:40);
Avg_circholes_soil=mean(circholes_soil_matrix)
Avg_circholes_clay=mean(circholes_clay_matrix)
Avg_circholes_rock=mean(circholes_rock_matrix)

%%
%difference between 4 row and no barrier
subplot(2,2,1)
[X4,Y4]=meshgrid(1:40,distance_4_row);
Z_comp_soil_4r=(20*log10(abs(V_soil_4_row)))-Vs4r;
surf(X4,Y4,Z_comp_soil_4r,'FaceAlpha',0.5)
ylim([23.5 30])
zlim([-20 30])
caxis([-30,20])
title('Difference in velocity levels between no barrier and 5 rows of 15cm radius holes at 1m center-center distance in soil')
c = colorbar;
c.Label.String = 'Velocity level difference in dB';
xlabel('Frequency (Hz)')
ylabel('Distance (m)')
zlabel('Velocity levels Z (dB)')
subplot(2,2,2)
%[X4,Y4]=meshgrid(1:40,distance_small_holes_tight);
Z_comp_clay_4r=(20*log10(abs(V_clay_4_row)))-Vc6;
surf(X4,Y4,Z_comp_clay_4r,'FaceAlpha',0.5)
ylim([23.5 30])
zlim([-10 25])
caxis([-30,20])
title('Difference in velocity levels between no barrier and 4 rows of 15cm radius holes at 1m center-center distance in clay')
c = colorbar;
c.Label.String = 'Velocity level difference in dB';
xlabel('Frequency (Hz)')
```

```
379 ylabel('Distance (m)')
380 zlabel('Velocity levels Z (dB)')
381 subplot(2,2,3.5)        %difference between large holes and no barrier -
        something is wrong
382 %[X4,Y4]=meshgrid(1:40,linspace(0,30,136));
383 Z_comp_rock_4r=(20*log10(abs(V_rock_4_row)))-Vr6;
384 surf(X4,Y4,Z_comp_rock_4r,'FaceAlpha',0.5)
385 ylim([23.5 30])
386 zlim([-5 5])
387 caxis([-20,10])
388 title('Difference in velocity levels between no barrier and 4 rows 15cm
        radius holes at 1m center-center distance in bedrock')
389 c = colorbar;
390 c.Label.String = 'Velocity level difference in dB';
391 xlabel('Frequency (Hz)')
392 ylabel('Distance (m)')
393 zlabel('Velocity levels Z (dB)')
394
395 % average reduction values
396 r4holes_soil_matrix=Z_comp_soil_4r(164:201,1:40);
397 r4holes_clay_matrix=Z_comp_clay_4r(164:201,1:40);
398 r4holes_rock_matrix=Z_comp_rock_4r(164:201,1:40);
399 Avg_4rholes_soil=mean(r4holes_soil_matrix)
400 Avg_4rholes_clay=mean(r4holes_clay_matrix)
401 Avg_4rholes_rock=mean(r4holes_rock_matrix)
402
403
404
405 %%
406 %difference between double row and no barrier
407 subplot(2,2,1)
408 [X4,Y4]=meshgrid(1:40,distance_dbl_row1);
409 [X5,Y5]=meshgrid(1:40,distance_dbl_row);
410 Z_comp_soil_2r=(20*log10(abs(V_soil_dbl_row)))-Vs2r1;
411 surf(X4,Y4,Z_comp_soil_2r,'FaceAlpha',0.5)
412 ylim([21.5 30])
413 zlim([-30 30])
414 caxis([-30,20])
415 title('Difference in velocity levels betwee

      n no barrier and 2 rows of 15cm radius holes at 1m center-center
      distance in soil')
416 c = colorbar;
417 c.Label.String = 'Velocity level difference in dB';
418 xlabel('Frequency (Hz)')
419 ylabel('Distance (m)')
```

```
zlabel('Velocity levels Z (dB)')
subplot(2,2,2)
%[X4,Y4]=meshgrid(1:40,distance_small_holes_tight);
Z_comp_clay_2r=(20*log10(abs(V_clay_dbl_row)))-Vc5;
surf(X4,Y4,Z_comp_clay_2r,'FaceAlpha',0.5)
ylim([21.5 30])
zlim([-15 20])
caxis([-30,20])
title('Difference in velocity levels between no barrier and 2 rows of 15cm radius holes at 1m center-center distance in clay')
c = colorbar;
c.Label.String = 'Velocity level difference in dB';
xlabel('Frequency (Hz)')
ylabel('Distance (m)')
zlabel('Velocity levels Z (dB)')
subplot(2,2,3.5)
%[X4,Y4]=meshgrid(1:40,linspace(0,30,136));
Z_comp_rock_2r=(20*log10(abs(V_rock_dbl_row)))-Vr5;
surf(X5,Y5,Z_comp_rock_2r,'FaceAlpha',0.5)
ylim([21.5 30])
zlim([-5 5])
caxis([-20,10])
title('Difference in velocity levels between no barrier and 2 rows 15cm radius holes at 1m center-center distance in bedrock')
c = colorbar;
c.Label.String = 'Velocity level difference in dB';
xlabel('Frequency (Hz)')
ylabel('Distance (m)')
zlabel('Velocity levels Z (dB)')

% average reduction values
dblrholes_soil_matrix=Z_comp_soil_2r(113:154,1:40);
dblrholes_clay_matrix=Z_comp_clay_2r(113:154,1:40);
dblrholes_rock_matrix=Z_comp_rock_2r(149:193,1:40);
Avg_2rholes_soil=mean(dblrholes_soil_matrix)
Avg_2rholes_clay=mean(dblrholes_clay_matrix)
Avg_2rholes_rock=mean(dblrholes_rock_matrix)



%%
%difference between large holes tight and no barrier
subplot(2,2,1)
[X4,Y4]=meshgrid(1:40,distance_large_holes_tight);
Z_comp_soil_lht=(20*log10(abs(V_soil_tight_large_holes)))-Vlht;
surf(X4,Y4,Z_comp_soil_lht,'FaceAlpha',0.5)
```

```
464 ylim([20.5 30])
465 zlim([-20 20])
466 caxis([-30,20])
467 title('Difference in velocity levels between no barrier and 30cm radius
        holes at 0.8m center-center distance in soil')
468 c = colorbar;
469 c.Label.String = 'Velocity level difference in dB';
470 xlabel('Frequency (Hz)')
471 ylabel('Distance (m)')
472 zlabel('Velocity levels Z (dB)')
473 subplot(2,2,2)
474 %[X4,Y4]=meshgrid(1:40,distance_small_holes_tight);
475 Z_comp_clay_lht=(20*log10(abs(V_clay_tight_large_holes)))-Vc4;
476 surf(X4,Y4,Z_comp_clay_lht,'FaceAlpha',0.5)
477 ylim([20.5 30])
478 zlim([-10 20])
479 caxis([-30,20])
480 title('Difference in velocity levels between no barrier and 30cm radius
        holes at 0.8m center-center distance in clay')
481 c = colorbar;
482 c.Label.String = 'Velocity level difference in dB';
483 xlabel('Frequency (Hz)')
484 ylabel('Distance (m)')
485 zlabel('Velocity levels Z (dB)')
486 subplot(2,2,3.5)       %difference between large holes and no barrier -
        something is wrong
487 %[X4,Y4]=meshgrid(1:40,linspace(0,30,136));
488 Z_comp_rock_lht=(20*log10(abs(V_rock_tight_large_holes)))-Vr4;
489 surf(X4,Y4,Z_comp_rock_lht,'FaceAlpha',0.5)
490 ylim([20.5 30])
491 zlim([-5 5])
492 caxis([-20,10])
493 title('Difference in velocity levels between no barrier and 15cm radius
        holes at 0.5m center-center distance in bedrock')
494 c = colorbar;
495 c.Label.String = 'Velocity level difference in dB';
496 xlabel('Frequency (Hz)')
497 ylabel('Distance (m)')
498 zlabel('Velocity levels Z (dB)')
499
500 % average reduction values
501 lthholes_soil_matrix=Z_comp_soil_lht(74:145,1:40);
502 lthholes_clay_matrix=Z_comp_clay_lht(74:145,1:40);
503 lthholes_rock_matrix=Z_comp_rock_lht(74:145,1:40);
504 Avg_lthholes_soil=mean(lthholes_soil_matrix)
505 Avg_lthholes_clay=mean(lthholes_clay_matrix)
```

```
506 Avg_lthholes_rock=mean(lthholes_rock_matrix)
507
508
509 %%
510
511
512 %difference between small holes tight and no barrier
513 subplot(2,2,1)
514 [X4,Y4]=meshgrid(1:40,distance_small_holes_tight);
515 Z_comp_soil_sht=(20*log10(abs(V_soil_tight_holes)))-Vsht;
516 surf(X4,Y4,Z_comp_soil_sht,'FaceAlpha',0.5)
517 ylim([20.5 30])
518 zlim([-20 20])
519 caxis([-30,20])
520 title('Difference in velocity levels between no barrier and 15cm radius
        holes at 0.5m center-center distance in soil')
521 c = colorbar;
522 c.Label.String = 'Velocity level difference in dB';
523 xlabel('Frequency (Hz)')
524 ylabel('Distance (m)')
525 zlabel('Velocity levels Z (dB)')
526 subplot(2,2,2)
527 %[X4,Y4]=meshgrid(1:40,distance_small_holes_tight);
528 Z_comp_clay_sht=(20*log10(abs(V_clay_tight_holes)))-Vc3;
529 surf(X4,Y4,Z_comp_clay_sht,'FaceAlpha',0.5)
530 ylim([20.5 30])
531 zlim([-10 20])
532 caxis([-30,20])
533 title('Difference in velocity levels between no barrier and 15cm radius
        holes at 0.5m center-center distance in clay')
534 c = colorbar;
535 c.Label.String = 'Velocity level difference in dB';
536 xlabel('Frequency (Hz)')
537 ylabel('Distance (m)')
538 zlabel('Velocity levels Z (dB)')
539 subplot(2,2,3.5)       %difference between large holes and no barrier -
        something is wrong
540 %[X4,Y4]=meshgrid(1:40,linspace(0,30,136));
541 Z_comp_rock_sht=(20*log10(abs(V_rock_tight_holes)))-Vr3;
542 surf(X4,Y4,Z_comp_rock_sht,'FaceAlpha',0.5)
543 ylim([20.5 30])
544 zlim([-5 5])
545 caxis([-20,10])
546 title('Difference in velocity levels between no barrier and 15cm radius
        holes at 0.5m center-center distance in bedrock')
547 c = colorbar;
```

```
548 c.Label.String = 'Velocity level difference in dB';
549 xlabel('Frequency (Hz)')
550 ylabel('Distance (m)')
551 zlabel('Velocity levels Z (dB)')
552
553
554 % average reduction values
555 sthholes_soil_matrix=Z_comp_soil_sht(105:163,1:40);
556 sthholes_clay_matrix=Z_comp_clay_sht(105:163,1:40);
557 sthholes_rock_matrix=Z_comp_rock_sht(105:163,1:40);
558 Avg_sthholes_soil=mean(sthholes_soil_matrix)
559 Avg_sthholes_clay=mean(sthholes_clay_matrix)
560 Avg_sthholes_rock=mean(sthholes_rock_matrix)
561
562
563 %% differences trench - DONE
564 %[X4,Y4]=meshgrid(1:40,linspace(0,30,154));
565 figure(19)              %difference between no barrier and trench
566 subplot(2,2,1)
567 Z_comp_soil1=(20*log10(abs(V_soil_trench)))-Vq;
568 surf(X,Y,Z_comp_soil1,'FaceAlpha',0.5)
569 ylim([20.5 30])
570 zlim([-35 20])
571 caxis([-30,10])
572 title('Difference in velocity levels between no barrier and trench in
      soil')
573 c = colorbar;
574 c.Label.String = 'Velocity level difference in dB';
575 xlabel('Frequency (Hz)')
576 ylabel('Distance (m)')
577 zlabel('Velocity levels Z (dB)')
578 subplot(2,2,2)          %difference between no barrier and trench in
      clay
579 Z_comp_clay1=(20*log10(abs(V_clay_trench)))-Vc1;
580 surf(X,Y,Z_comp_clay1,'FaceAlpha',0.5)
581 ylim([20.5 30])
582 zlim([-30 20])
583 caxis([-30,10])
584 title('Difference in velocity levels between no barrier and trench in
      clay')
585 c = colorbar;
586 c.Label.String = 'Velocity level difference in dB';
587 xlabel('Frequency (Hz)')
588 ylabel('Distance (m)')
589 zlabel('Velocity levels Z (dB)')
590 subplot(2,2,3.5)          %difference between no barrier and trench
```

```
Z_comp_rock1=(20*log10(abs(V_rock_trench)))-Vr1;
surf(X,Y,Z_comp_rock1,'FaceAlpha',0.5)
ylim([20.5 30])
zlim([-5 5])
caxis([-20,10])
title('Difference in velocity levels between no barrier and trench in
    rock')
c = colorbar;
c.Label.String = 'Velocity level difference in dB';
xlabel('Frequency (Hz)')
ylabel('Distance (m)')
zlabel('Velocity levels Z (dB)')


% average reduction values
trench_soil_matrix=Z_comp_soil1(109:154,1:40);
trench_clay_matrix=Z_comp_clay1(109:154,1:40);
trench_rock_matrix=Z_comp_rock1(109:154,1:40);
Avg_trench_soil=mean(trench_soil_matrix)
Avg_trench_clay=mean(trench_clay_matrix)
Avg_trench_rock=mean(trench_rock_matrix)

%%
% differences holes - DONE

figure(23)          %difference between holes and no barrier
subplot(2,2,1)
Z_comp_soil2=(20*log10(abs(V_soil_holes)))-Vq;
surf(X,Y,Z_comp_soil2,'FaceAlpha',0.5)
ylim([20.5 30])
zlim([-20 20])
caxis([-30,20])
title('Difference in velocity levels between soil with no barrier and
    15cm holes')
c = colorbar;
c.Label.String = 'Velocity level difference in dB';
xlabel('Frequency (Hz)')
ylabel('Distance (m)')
zlabel('Velocity levels Z (dB)')
subplot(2,2,2)
Z_comp_clay2=(20*log10(abs(V_clay_holes)))-Vc1;
surf(X,Y,Z_comp_clay2,'FaceAlpha',0.5)
ylim([20.5 30])
zlim([-5 20])
caxis([-20,20])
title('Difference in velocity levels between clay with no barrier and
```

```
    15cm holes')
c = colorbar;
c.Label.String = 'Velocity level difference in dB';
xlabel('Frequency (Hz)')
ylabel('Distance (m)')
zlabel('Velocity levels Z (dB)')
subplot(2,2,3.5)
%figure(26)          %difference between holes and no barrier
Z_comp_rock2=(20*log10(abs(V_rock_holes)))-Vr1;
surf(X,Y,Z_comp_rock2,'FaceAlpha',0.5)
ylim([20.5 30])
zlim([-5 5])
caxis([-20,0])
title('Difference in velocity levels between rock with no barrier and
    15cm holes')
c = colorbar;
c.Label.String = 'Velocity level difference in dB';
xlabel('Frequency (Hz)')
ylabel('Distance (m)')
zlabel('Velocity levels Z (dB)')


% average reduction values
holes_soil_matrix=Z_comp_soil2(109:154,1:40);
holes_clay_matrix=Z_comp_clay2(109:154,1:40);
holes_rock_matrix=Z_comp_rock2(109:154,1:40);
Avg_holes_soil=mean(holes_soil_matrix)
Avg_holes_clay=mean(holes_clay_matrix)
Avg_holes_rock=mean(holes_rock_matrix)




%% Large holes difference

figure(24)          %difference between large holes and no barrier
subplot(2,2,1)
[X4,Y4]=meshgrid(1:40,distance_large_holes);
Z_comp_soil3=(20*log10(abs(V_soil_large_holes)))-Vq1;
surf(X4,Y4,Z_comp_soil3,'FaceAlpha',0.5)
ylim([20.5 30])
zlim([-20 20])
caxis([-30,20])
title('Difference in velocity levels between no barrier and 30cm radius
    holes in soil')
c = colorbar;
```

```
678 c.Label.String = 'Velocity level difference in dB';
679 xlabel('Frequency (Hz)')
680 ylabel('Distance (m)')
681 zlabel('Velocity levels Z (dB)')
682 subplot(2,2,2)
683 [X4,Y4]=meshgrid(1:40,distance_large_holes);
684 Z_comp_clay3=(20*log10(abs(V_clay_large_holes)))-Vc2;
685 surf(X4,Y4,Z_comp_clay3,'FaceAlpha',0.5)
686 ylim([21.5 30])
687 zlim([-5 20])
688 caxis([-30,20])
689 title('Difference in velocity levels between no barrier and 30cm radius
        holes in clay')
690 c = colorbar;
691 c.Label.String = 'Velocity level difference in dB';
692 xlabel('Frequency (Hz)')
693 ylabel('Distance (m)')
694 zlabel('Velocity levels Z (dB)')
695 subplot(2,2,3.5)       %difference between large holes and no barrier -
        something is wrong
696 %[X4,Y4]=meshgrid(1:40,linspace(0,30,136));
697 Z_comp_rock3=(20*log10(abs(V_rock_large_holes)))-Vr2;
698 surf(X4,Y4,Z_comp_rock3,'FaceAlpha',0.5)
699 ylim([21.5 30])
700 zlim([-5 5])
701 caxis([-20,10])
702 title('Difference in velocity levels between no barrier and 30cm radius
        holes in bedrock')
703 c = colorbar;
704 c.Label.String = 'Velocity level difference in dB';
705 xlabel('Frequency (Hz)')
706 ylabel('Distance (m)')
707 zlabel('Velocity levels Z (dB)')
708
709 % average reduction values
710 Lholes_soil_matrix=Z_comp_soil3(99:136,1:40);
711 Lholes_clay_matrix=Z_comp_clay3(99:136,1:40);
712 Lholes_rock_matrix=Z_comp_rock3(99:136,1:40);
713 Avg_Lholes_soil=mean(Lholes_soil_matrix)
714 Avg_Lholes_clay=mean(Lholes_clay_matrix)
715 Avg_Lholes_rock=mean(Lholes_rock_matrix)
716
717
718 %% combined 3d figure
719 figure(16)
720 [X,Y]=meshgrid(1:40,linspace(0,30,154));
```

```
721 Z=20*log10(abs(V_soil_trench));
722 surf(X,Y,Z,'FaceAlpha',0.5)
723 hold on
724 [X1,Y1]=meshgrid(1:40,linspace(0,30,64));
725 Z_wo=20*log10(abs(V_soil_wo_barrier));
726 surf(X1,Y1,Z_wo,'FaceAlpha',0.5)
727 title('Soil with trench')
728 xlabel('Frequency (Hz)')
729 ylabel('Distance (m)')
730 zlabel('Velocity levels Z (dB)')
731
732
733
734 %% inverted combined 3d figure
735
736 %[X1,Y1]=meshgrid(1:40,linspace(0,30,64));
737 figure(17)
738 Z_comp=-(20*log10(abs(V_soil_holes))-20*log10(abs(V_soil_trench)));
739 surf(X,Y,Z_comp,'FaceAlpha',0.5)
740 ylim([22 30])
741 zlim([-40 40])
742 caxis([-40,40])
743 title('Soil with trench')
744 xlabel('Frequency (Hz)')
745 ylabel('Distance (m)')
746 zlabel('Velocity levels Z (dB)')
747
748
749
750
751 % Velocity level plots
752
753 %% separated figures without barrier - DONE
754
755 figure(6)                %velocity levels Z soil without barrier
756 subplot(2,2,1)
757 [X1,Y1]=meshgrid(1:40,linspace(0,30,64));
758 Z_wo=20*log10(abs(V_soil_wo_barrier));
759 surf(X1,Y1,Z_wo,'FaceAlpha',0.5)
760 s.EdgeColor = 'none';
761 title('Soil without barrier')
762 c = colorbar;
763 c.Label.String = 'Velocity level in dB';
764 xlabel('Frequency (Hz)')
765 ylabel('Distance (m)')
766 zlabel('Velocity levels Z (dB)')
```

```
767 subplot(2,2,2)
768 %figure(10)                %velocity levels Z clay
769 %[X,Y]=meshgrid(1:40,linspace(0,30,64));
770 Z=20*log10(abs(V_clay_wo_barrier));
771 surf(X1,Y1,Z,'FaceAlpha',0.5)
772 s.EdgeColor = 'none';
773 title('Clay without barrier')
774 c = colorbar;
775 c.Label.String = 'Velocity level in dB';
776 xlabel('Frequency (Hz)')
777 ylabel('Distance (m)')
778 zlabel('Velocity levels Z (dB)')
779 subplot(2,2,3.5)
780 %figure(13)          %bedrock without barrier
781 %[X,Y]=meshgrid(1:40,linspace(0,30,64));
782 Z=20*log10(abs(V_rock_wo_barrier));
783 surf(X1,Y1,Z,'FaceAlpha',0.5)
784 s.EdgeColor = 'none';
785 title('Bedrock without barrier')
786 c = colorbar;
787 c.Label.String = 'Velocity level in dB';
788 xlabel('Frequency (Hz)')
789 ylabel('Distance (m)')
790 zlabel('Velocity levels Z (dB)')
791 %% double row -
792
793 figure(10)                %velocity levels Z soil with dbl row
794 subplot(2,2,1)
795 [X8,Y8]=meshgrid(1:40,distance_dbl_row1);
796 [X9,Y9]=meshgrid(1:40,distance_dbl_row);
797 Z_2r_s=20*log10(abs(V_soil_dbl_row));
798 surf(X8,Y8,Z_2r_s,'FaceAlpha',0.5)
799 s.EdgeColor = 'none';
800 title('Soil with 2 rows of 15cm holes, center-center distance 1m')
801 c = colorbar;
802 c.Label.String = 'Velocity level in dB';
803 xlabel('Frequency (Hz)')
804 ylabel('Distance (m)')
805 zlabel('Velocity levels Z (dB)')
806 subplot(2,2,2)
807 Z_2r_cl=20*log10(abs(V_clay_dbl_row));
808 surf(X8,Y8,Z_2r_cl,'FaceAlpha',0.5)
809 s.EdgeColor = 'none';
810 title('Clay with 2 rows of 15cm holes, center-center distance 1m')
811 xlabel('Frequency (Hz)')
812 ylabel('Distance (m)')
```

```
zlabel('Velocity levels Z (dB)')
c = colorbar;
c.Label.String = 'Velocity level in dB';
subplot(2,2,3.5)
Z_2r_r=20*log10(abs(V_rock_dbl_row));
surf(X9,Y9,Z_2r_r,'FaceAlpha',0.5)
s.EdgeColor = 'none';
title('Rock with 2 rows of 15cm holes, center-center distance 1m')
xlabel('Frequency (Hz)')
ylabel('Distance (m)')
zlabel('Velocity levels Z (dB)')
c = colorbar;
c.Label.String = 'Velocity level in dB';


%%
% 4 row

figure(10)                %velocity levels Z soil with 4 row
subplot(2,2,1)
[X3,Y3]=meshgrid(1:40,distance_4_row);
Z_4r_s=20*log10(abs(V_soil_4_row));
surf(X3,Y3,Z_4r_s,'FaceAlpha',0.5)
s.EdgeColor = 'none';
title('Soil with 4 rows of 15cm holes, center-center distance 1m')
xlabel('Frequency (Hz)')
ylabel('Distance (m)')
zlabel('Velocity levels Z (dB)')
c = colorbar;
c.Label.String = 'Velocity level in dB';
subplot(2,2,2)
Z_4r_cl=20*log10(abs(V_clay_4_row));
surf(X3,Y3,Z_4r_cl,'FaceAlpha',0.5)
s.EdgeColor = 'none';
title('Clay with 2 rows of 15cm holes, center-center distance 1m')
xlabel('Frequency (Hz)')
ylabel('Distance (m)')
zlabel('Velocity levels Z (dB)')
c = colorbar;
c.Label.String = 'Velocity level in dB';
subplot(2,2,3.5)
Z_4r_r=20*log10(abs(V_rock_4_row));
surf(X3,Y3,Z_4r_r,'FaceAlpha',0.5)
s.EdgeColor = 'none';
title('Rock with 2 rows of 15cm holes, center-center distance 1m')
xlabel('Frequency (Hz)')
```

```
ylabel('Distance (m)')
zlabel('Velocity levels Z (dB)')
c = colorbar;
c.Label.String = 'Velocity level in dB';
%%
% tight large holes

figure(10)                  %velocity levels Z soil with 4 row
subplot(2,2,1)
[X3,Y3]=meshgrid(1:40,distance_large_holes_tight);
Z_tlh_s=20*log10(abs(V_soil_tight_large_holes));
surf(X3,Y3,Z_tlh_s,'FaceAlpha',0.5)
s.EdgeColor = 'none';
title('Velocity levels in soil with 1 row of 30cm holes, center-center
    distance 0.8m')
xlabel('Frequency (Hz)')
ylabel('Distance (m)')
zlabel('Velocity levels Z (dB)')
c = colorbar;
c.Label.String = 'Velocity level in dB';
subplot(2,2,2)
Z_tlh_cl=20*log10(abs(V_clay_tight_large_holes));
surf(X3,Y3,Z_tlh_cl,'FaceAlpha',0.5)
s.EdgeColor = 'none';
title('Velocity levels in clay with 1 row of 30cm holes, center-center
    distance 0.8m')
xlabel('Frequency (Hz)')
ylabel('Distance (m)')
zlabel('Velocity levels Z (dB)')
c = colorbar;
c.Label.String = 'Velocity level in dB';
subplot(2,2,3.5)
Z_tlh_r=20*log10(abs(V_rock_tight_large_holes));
surf(X3,Y3,Z_tlh_r,'FaceAlpha',0.5)
s.EdgeColor = 'none';
title('Velocity levels in rock with 1 row of 30cm holes, center-center
    distance 0.8m')
xlabel('Frequency (Hz)')
ylabel('Distance (m)')
zlabel('Velocity levels Z (dB)')
c = colorbar;
c.Label.String = 'Velocity level in dB';

%%

% tight small holes
```

```
%velocity levels Z soil
subplot(2,2,1)
[X3,Y3]=meshgrid(1:40,distance_small_holes_tight);
Z_tsm_s=20*log10(abs(V_soil_tight_holes));
surf(X3,Y3,Z_tsm_s,'FaceAlpha',0.5)
s.EdgeColor = 'none';
title('Velocity levels in soil with 1 row of 15cm holes, center-center
    distance 0.5m')
xlabel('Frequency (Hz)')
ylabel('Distance (m)')
zlabel('Velocity levels Z (dB)')
c = colorbar;
c.Label.String = 'Velocity level in dB';
subplot(2,2,2)
Z_tsm_cl=20*log10(abs(V_clay_tight_holes));
surf(X3,Y3,Z_tsm_cl,'FaceAlpha',0.5)
s.EdgeColor = 'none';
title('Velocity levels in clay with 1 row of 15cm holes, center-center
    distance 0.5m')
xlabel('Frequency (Hz)')
ylabel('Distance (m)')
zlabel('Velocity levels Z (dB)')
c = colorbar;
c.Label.String = 'Velocity level in dB';
subplot(2,2,3.5)
Z_tsm_r=20*log10(abs(V_rock_tight_holes));
surf(X3,Y3,Z_tsm_r,'FaceAlpha',0.5)
s.EdgeColor = 'none';
title('Velocity levels in rock with 1 row of 15cm holes, center-center
    distance 0.5m')
xlabel('Frequency (Hz)')
ylabel('Distance (m)')
zlabel('Velocity levels Z (dB)')
c = colorbar;
c.Label.String = 'Velocity level in dB';

%% large holes
figure(9)                %velocity levels Z soil with large holes
subplot(2,2,1)
[X3,Y3]=meshgrid(1:40,distance_large_holes);
Z_lh=20*log10(abs(V_soil_large_holes));
surf(X3,Y3,Z_lh,'FaceAlpha',0.5)
s.EdgeColor = 'none';
title('Soil with 30cm holes, cc distance 1m')
xlabel('Frequency (Hz)')
ylabel('Distance (m)')
```

```
945 zlabel('Velocity levels Z (dB)')
946 subplot(2,2,2)
947 Z_lh_cl=20*log10(abs(V_clay_large_holes));
948 surf(X3,Y3,Z_lh_cl,'FaceAlpha',0.5)
949 s.EdgeColor = 'none';
950 title('Clay with 30cm holes, cc distance 1m')
951 xlabel('Frequency (Hz)')
952 ylabel('Distance (m)')
953 zlabel('Velocity levels Z (dB)')
954 subplot(2,2,3.5)
955 Z_lh_r=20*log10(abs(V_rock_large_holes));
956 surf(X3,Y3,Z_lh_r,'FaceAlpha',0.5)
957 s.EdgeColor = 'none';
958 title('Rock with 30cm holes, cc distance 1m')
959 xlabel('Frequency (Hz)')
960 ylabel('Distance (m)')
961 zlabel('Velocity levels Z (dB)')
962
963
964 %% SINGLE ROW holes - DONE
965 figure(8)                %velocity levels Z soil with holes
966 [X2,Y2]=meshgrid(1:40,distance_trench);
967 subplot(2,2,1)
968 Z_wo=20*log10(abs(V_soil_holes));
969 surf(X,Y,Z_wo,'FaceAlpha',0.5)
970 s.EdgeColor = 'none';
971 title('Soil with 15cm radius holes, cc distance 1m, depth 9m')
972 xlabel('Frequency (Hz)')
973 ylabel('Distance (m)')
974 zlabel('Velocity levels Z (dB)')
975 c = colorbar;
976 %c.Label.String = 'Velocity level difference in dB';
977 %figure(12)               %clay with holes
978 %[X,Y]=meshgrid(1:40,linspace(0,30,64));
979 subplot(2,2,2)
980 Zclay=20*log10(abs(V_clay_holes));
981 surf(X,Y,Zclay,'FaceAlpha',0.5)
982 s.EdgeColor = 'none';
983 title('Clay with 15cm radius holes, cc distance 1m, depth 9m')
984 xlabel('Frequency (Hz)')
985 ylabel('Distance (m)')
986 zlabel('Velocity levels Z (dB)')
987 c = colorbar;
988 %c.Label.String = 'Velocity level difference in dB';
989 %figure(15)          %bedrock with holes
990 %[X,Y]=meshgrid(1:40,linspace(0,30,64));
```

```
991  subplot(2,2,3.5)
992  Zrock=20*log10(abs(V_rock_holes));
993  surf(X,Y,Zrock,'FaceAlpha',0.5)
994  s.EdgeColor = 'none';
995  title('Bedrock with 15cm radius holes, cc distance 1m, depth 9m')
996  xlabel('Frequency (Hz)')
997  ylabel('Distance (m)')
998  zlabel('Velocity levels Z (dB)')
999  c = colorbar;
1000 %c.Label.String = 'Velocity level difference in dB';
1001
1002
1003 %% trench - DONE
1004
1005 figure(7)                %Velocity levels Z with trench
1006 subplot(2,2,1)
1007 [X,Y]=meshgrid(1:40,distance_trench);
1008 Z=20*log10(abs(V_soil_trench));
1009 surf(X,Y,Z,'FaceAlpha',0.5)
1010 s.EdgeColor = 'none';
1011 title('Soil with 6m deep, 0.5m wide trench')
1012 c = colorbar;
1013 c.Label.String = 'Velocity level in dB';
1014 xlabel('Frequency (Hz)')
1015 ylabel('Distance (m)')
1016 zlabel('Velocity levels Z (dB)')
1017 subplot(2,2,2)           %velocity levels Z clay w trench
1018 Z=20*log10(abs(V_clay_trench));
1019 surf(X,Y,Z,'FaceAlpha',0.5)
1020 s.EdgeColor = 'none';
1021 title('Clay with 6m deep, 0.5m wide trench')
1022 c = colorbar;
1023 c.Label.String = 'Velocity level in dB';
1024 xlabel('Frequency (Hz)')
1025 ylabel('Distance (m)')
1026 zlabel('Velocity levels Z (dB)')
1027 subplot(2,2,3.5)         %bedrock with trench
1028 %[X,Y]=meshgrid(1:40,linspace(0,30,64));
1029 Z=20*log10(abs(V_rock_trench));
1030 surf(X,Y,Z,'FaceAlpha',0.5)
1031 s.EdgeColor = 'none';
1032 title('Bedrock with 6m deep, 0.5m wide trench')
1033 c = colorbar;
1034 c.Label.String = 'Velocity level in dB';
1035 xlabel('Frequency (Hz)')
1036 ylabel('Distance (m)')
```

```
1037 zlabel('Velocity levels Z (dB)')
1038
1039 %%
1040
1041 figure(6)                %velocity levels Z soil without barrier
1042 subplot(2,2,1)
1043 [X1,Y1]=meshgrid(1:40,distance_circ);
1044 Z_circ=20*log10(abs(V_soil_circular_barrier));
1045 surf(X1,Y1,Z_circ,'FaceAlpha',0.5)
1046 s.EdgeColor = 'none';
1047 title('Soil with circular array of cylinders')
1048 c = colorbar;
1049 c.Label.String = 'Velocity level in dB';
1050 xlabel('Frequency (Hz)')
1051 ylabel('Distance (m)')
1052 zlabel('Velocity levels Z (dB)')
1053 subplot(2,2,2)
1054 %figure(10)                %velocity levels Z clay
1055 %[X,Y]=meshgrid(1:40,linspace(0,30,64));
1056 Zc_circ=20*log10(abs(V_clay_circular_barrier));
1057 surf(X1,Y1,Zc_circ,'FaceAlpha',0.5)
1058 s.EdgeColor = 'none';
1059 title('Clay with circular array of cylinders')
1060 c = colorbar;
1061 c.Label.String = 'Velocity level in dB';
1062 xlabel('Frequency (Hz)')
1063 ylabel('Distance (m)')
1064 zlabel('Velocity levels Z (dB)')
1065 subplot(2,2,3.5)
1066 %figure(13)           %bedrock without barrier
1067 %[X,Y]=meshgrid(1:40,linspace(0,30,64));
1068 Zr_circ=20*log10(abs(V_rock_circular_barrier));
1069 surf(X1,Y1,Zr_circ,'FaceAlpha',0.5)
1070 s.EdgeColor = 'none';
1071 title('Bedrock with circular array of cylinders')
1072 c = colorbar;
1073 c.Label.String = 'Velocity level in dB';
1074 xlabel('Frequency (Hz)')
1075 ylabel('Distance (m)')
1076 zlabel('Velocity levels Z (dB)')
1077
1078
1079 %Individual frequencies
1080
1081 %%
1082 %soil individual frequencies
```

```
x1=20;
y1=-110;
x2=20;
y2=-190;

figure(1)                %velocity levels Z
subplot(1,2,1)
semilogy(d_trench, 20*log10(abs(V_soil_trench(:,40))),':')
hold on
semilogy(distance_wo_trench, 20*log10(abs(V_soil_wo_barrier(:,40))))
hold on
%semilogy(d_trench, 20*log10(abs(V_soil_holes(:,18))), '--','Linewidth',1.5)
hold on
%semilogy(d_large_holes, 20*log10(abs(V_soil_large_holes(:,18))),'--')
grid on
ylimit=get(gca,'Ylim')
plot([20 20],ylimit,'Linewidth',2)
title("Soil; P wave speed 1400 m/s , S wave speed 115 m/s")
legend("Trench","No trench","15cm radius holes, 1m cc",'30cm radius holes, 1m cc', "Trench position")
xlabel("Distance from source (m)")
ylabel("Velocity amplitude levels (dB)")
subplot(1,2,2)          %velocity levels X
semilogy(d_trench, 20*log10(abs(V_X_soil_trench(:,18))),':')
hold on
semilogy(distance_wo_trench, 20*log10(abs(V_X_soil_wo_barrier(:,18))))
hold on
semilogy(d_trench, 20*log10(abs(V_x_soil_holes(:,18))),'--')
hold on
semilogy(d_large_holes, 20*log10(abs(V_X_soil_large_holes(:,18))),'--')
grid on
ylimit=get(gca,'Ylim')
plot([20 20],ylimit,'Linewidth',2)
title("Soil velocity levels in X; P wave speed 1400 m/s , S wave speed 115 m/s")
legend("Trench","No trench","15cm radius holes, 1m cc","30cm radius holes, 1m cc", "Trench position")
xlabel("Distance from source (m)")
ylabel("Velocity amplitude levels (dB)")


%% clay individual frequencies
%clay
figure(2)                %velocity levels Z
subplot(1,2,1)
```

```
1125 semilogy(d_trench, 20*log10(abs(V_clay_trench(:,5))),':');
1126 hold on
1127 semilogy(distance_wo_trench, 20*log10(abs(V_clay_wo_barrier(:,5))))
1128 hold on
1129 semilogy(d_trench, 20*log10(abs(V_clay_holes(:,5))),'--','Linewidth'
     ,1.5)
1130 hold on
1131 semilogy(d_large_holes, 20*log10(abs(V_clay_large_holes(:,5))),'--')
1132 ylimit=get(gca,'Ylim')
1133 plot([20 20],ylimit,'Linewidth',2)
1134 title("Clay; P wave speed , S wave speed ")
1135 legend("Trench","No Trench","15cm radius holes, 1m cc","30cm radius
     holes","trench position",'Location','Northwest')
1136 xlabel("Distance from source (m)")
1137 ylabel("Velocity amplitude levels (dB)")
1138 subplot(1,2,2)                    %velocity levels X
1139 semilogy(d_trench, 20*log10(abs(V_X_clay_trench(:,18))),':')
1140 hold on
1141 semilogy(distance_wo_trench, 20*log10(abs(V_X_clay_wo_barrier(:,18))))
1142 hold on
1143 semilogy(d_large_holes, 20*log10(abs(V_X_clay_large_holes(:,18))),'--')
1144 grid on
1145 ylimit=get(gca,'Ylim')
1146 plot([20 20],ylimit,'Linewidth',2)
1147 title("Clay velocity levels X; P wave speed , S wave speed ")
1148 legend("Trench","No trench","30cm radius holes, 1m cc distance", "
     Trench position",'Location','Northwest')
1149 xlabel("Distance from source (m)")
1150 ylabel("Velocity amplitude levels (dB)")
1151
1152 %15 Hz looks weird
1153 %slight reduction after 30 hz
1154
1155 %% bedrock individual frequencies
1156 %bedrock
1157 figure(5)                %bedrock
1158 subplot(1,2,1)
1159 semilogy(d_trench, 20*log10(abs(V_rock_trench(:,35))),':');
1160 hold on
1161 semilogy(distance_wo_trench, 20*log10(abs(V_rock_wo_barrier(:,35))))
1162 hold on
1163 semilogy(d_trench, 20*log10(abs(V_rock_holes(:,35))),'--','Linewidth'
     ,1.5)
1164 hold on
1165 semilogy(d_large_holes, 20*log10(abs(V_rock_large_holes(:,35))),'--')
1166 ylimit=get(gca,'Ylim')
```

```
1167 plot([20 20],ylimit,'Linewidth',2)
1168 title("Bedrock velocity levels Z; P wave speed , S wave speed ")
1169 legend("Trench","No Trench","15cm radius holes, 1m cc distance","30cm
     radius holes, 1m cc distance", "Trench position")
1170 xlabel("Distance from source (m)")
1171 ylabel("Velocity amplitude levels (dB)")
1172 subplot(1,2,2)
1173 semilogy(d_large_holes, 20*log10(abs(V_X_rock_large_holes(:,4))),'--');
1174 hold on
1175 semilogy(distance_wo_trench, 20*log10(abs(V_X_bedrock_wo_barrier(:,4)))
     )
1176 hold on
1177 semilogy(d_trench, 20*log10(abs(V_x_rock_holes(:,4))),'--','Linewidth'
     ,1.5)
1178 ylimit=get(gca,'Ylim')
1179 plot([20 20],ylimit,'Linewidth',2)
1180 title("Bedrock velocity levels X; P wave speed , S wave speed ")
1181 legend("30cm radius holes, 1m cc distance","No Trench","15cm radius
     holes, 1m cc distance","Trench position")
1182 xlabel("Distance from source (m)")
1183 ylabel("Velocity amplitude levels (dB)")
```